



# A performance analysis of multi-satellite joint geolocation\*

Ding WANG<sup>†‡1,2</sup>, Shuai WEI<sup>1</sup>, Ying WU<sup>2</sup>

<sup>(1)</sup>National Digital Switching System Engineering & Technological Research Center, Zhengzhou 450002, China)

<sup>(2)</sup>Zhengzhou Information Science and Technology Institute, Zhengzhou 450002, China)

<sup>†</sup>E-mail: wang\_ding814@aliyun.com

Received Sept. 4, 2015; Revision accepted Apr. 28, 2016; Crosschecked Nov. 8, 2016

**Abstract:** Determining the position of an emitter on Earth by using a satellite cluster has many important applications, such as in navigation, surveillance, and remote sensing. However, in realistic situations, a number of factors, such as errors in the measurement of signal parameters, uncertainties regarding the position of satellites, and errors in the location of calibration sources, are known to degrade the accuracy of target localization in satellite geolocation systems. We systematically analyze the performance of multi-satellite joint geolocation based on time difference of arrival (TDOA) measurements. The theoretical analysis starts with Cramér–Rao bound (CRB) derivations for four localization scenarios under an altitude constraint and Gaussian noise assumption. In scenario 1, only the TDOA measurement errors of the emitting source are considered and the satellite positions are assumed to be perfectly estimated. In scenario 2, both the TDOA measurement errors and satellite position uncertainties are taken into account. Scenario 3 assumes that some calibration sources with accurate position information are used to mitigate the influence of satellite position perturbations. In scenario 4, several calibration sources at inaccurate locations are used to alleviate satellite position errors in target localization. Through comparing the CRBs of the four localization scenarios, some valuable insights are gained into the effects of various error sources on the estimation performance. Two kinds of location mean-square errors (MSE) expressions under the altitude constraint are derived through first-order perturbation analysis and the Lagrange method. The first location MSE provides the theoretical prediction when an estimator assumes that the satellite locations are accurate but in fact have errors. The second location MSE provides the localization accuracy if an estimator assumes that the known calibration source locations are precise while in fact erroneous. Simulation results are included to verify the theoretical analysis.

**Key words:** Satellite geolocation, Time difference of arrival (TDOA), Cramér–Rao bound (CRB), Calibration sources, Performance analysis

<http://dx.doi.org/10.1631/FITEE.1500285>

**CLC number:** TN911.7

## 1 Introduction

Determining the location of an object on the surface of the Earth (geolocation) has attracted extensive attention due to its importance in many applications such as navigation, surveillance, maritime rescue, and remote sensing. A localization system

generally consists of a number of spatially well separated receivers (sensors) that capture the radiated or reflected signals from an emitter. In particular, locating an object on the Earth by using a satellite cluster has become popular in recent years due to the wide area of coverage and high precision of localization (Ha and Robertson, 1987; Bardelli *et al.*, 1995; Haworth *et al.*, 1997; Lee *et al.*, 2000). The signal parameters commonly used for satellite geolocation include time difference of arrival (TDOA), frequency difference of arrival (FDOA), time of arrival (TOA), frequency of arrival (FOA), and azimuth of arrival (AOA). In general, if the altitude of an emitter on the Earth is known or can be measured with an altimeter, two measurements are enough to determine the target

<sup>‡</sup> Corresponding author

\* Project supported by the National Natural Science Foundation of China (No. 61201381), the Future Development Foundation of Zhengzhou Information Science and Technology Institute (No. YP12JJ202057), China Postdoctoral Science Foundation (No. 2016M592989), and the Outstanding Youth Foundation of Information Engineering University (No. 2016603201)

ORCID: Ding WANG, <http://orcid.org/0000-0001-6533-9206>

© Zhejiang University and Springer-Verlag Berlin Heidelberg 2016

location. In a dual-satellite geolocation system, a pair of TDOA/FDOA (Ho and Chan, 1997; Pattison and Chou, 2000; Wu and Luo, 2009; Mušicki *et al.*, 2010) or TOA/FOA (Mason, 2004) measurements of the transmitted signal impinging on two receivers is obtained to geolocalize the target, along with an altitude constraint; in a tri-satellite geolocation system, two TDOA (Ho and Chan, 1993) or FDOA (Witzgall, 2014) measurements of the radiated signal received by three sensors are estimated to geolocate the emitter with the altitude knowledge of the emitter. Clearly, if more satellites are used to form an overdetermined set of equations, the localization accuracy can be further increased (Niezgoda and Ho, 1994; Ho and Chan, 1997; Musicki and Koch, 2008; Yang *et al.*, 2011).

The position determination from the measurements is equivalent to solving a set of nonlinear equations relating signal parameters to position information. During recent decades, a number of localization methods have been proposed. Some are iterative algorithms (such as Taylor-series algorithms (Kovavisaruch and Ho, 2005; Lu and Ho, 2006a) and constrained total least squares algorithms (Yang *et al.*, 2010; Yu *et al.*, 2012)) that require proper initial solution guesses, and others are closed-form solutions (such as the quadratic constraint least square solution (Huang *et al.*, 2001; Cheung *et al.*, 2006) and the two-step weighted least square solution (Ho and Xu, 2004; Ho *et al.*, 2007)) that are more computationally efficient. Most of these algorithms are able to reach their corresponding Cramér–Rao bound (CRB) accuracy under a moderate signal-to-noise ratio (SNR). However, for a satellite geolocation scenario, the altitude of the emitter may be known in advance. For example, an object on the Earth’s surface has zero altitude at sea level. Evidently, it is advantageous to include this constraint to increase the location accuracy, and the localization algorithms mentioned above can be suitably modified to incorporate this prior knowledge. Ho and Chan (1997) developed a closed-form geolocation solution with the altitude constraint, and Ding (2014) developed a constrained Taylor-series location algorithm with altitude knowledge. Both of these geolocation algorithms have CRB accuracies at a moderate noise level.

In engineering applications, there are two major factors limiting geolocation accuracy: the measurement errors of the signal parameters, and the satellite

position and velocity uncertainties. Measurement errors can be reduced by increasing the signal observation period. Satellite position and velocity uncertainties can be restrained by incorporating the statistical distribution of the receiver position and velocity errors into the localization algorithms (Ho *et al.*, 2007; Ding, 2014), or eliminated by applying calibration sources at an accurate location (Ho and Yang, 2008; Yang and Ho, 2010a). The use of calibration sources at precise positions can significantly reduce the loss of accuracy in source localization when the available receiver positions and velocities have random errors. However, a more realistic situation is that the exact locations of the calibration sources are not available (Yang and Ho, 2010b). Inaccurate knowledge of the calibration emitter location can be found quite often in practice. For example, the calibration emitter may be on a moving platform, such as a land vehicle or an unmanned aerial vehicle (UAV) whose position cannot be obtained precisely. Alternatively, the emitter for calibration may be unintentional. In Yang and Ho (2010b), the amount of reduction in localization accuracy due to calibration position errors was derived through CRB analysis. They concluded that the penalty could be very high if an estimator assumes that the known calibration source locations are precise while in fact erroneous. Fortunately, they also showed that compared to a scenario with no calibration emitters, the use of calibration sources can always improve the location accuracy, regardless of whether the calibration source positions are perfectly obtained.

Note that although there have been many studies on the effects of various error sources on emitter location accuracy (Lu and Ho, 2006b; Ho *et al.*, 2007; Ho and Yang, 2008; Yang and Ho, 2010b), these results cannot be readily extended to a satellite geolocation scenario with an altitude constraint. However, due to the importance and extensive use of satellite geolocation systems, a detailed performance analysis is essential to identify the level of accuracy which each variable must be determined to achieve the desired geolocation outcome. Note that although some analyses have been carried out on satellite geolocation (Ho and Chan, 1997; Wu and Luo, 2009; Pattison and Chou, 2000), they were not sufficiently systematic and comprehensive. For example, the effects of the calibration source were not taken into account,

only one or two error sources were considered, and comparisons of their performance were insufficient. We provide a more comprehensive and detailed theoretical analysis on satellite geolocation. Without loss of generality, TDOA based multi-satellite geolocation is used as an example for illustration. The theoretical analysis starts with CRB derivation for four geolocation scenarios under an altitude constraint and Gaussian noise assumption. In scenario 1, only TDOA measurement errors of the emitting source are accounted for, and the satellite positions are assumed to be perfectly obtained. In scenario 2, TDOA measurement errors and the satellite position perturbations are simultaneously considered. Scenario 3 assumes that some calibration sources with accurate position information are used to restrain the effects of satellite position perturbations; In scenario 4, several calibration sources at inaccurate positions are employed to alleviate satellite position uncertainties in target localization. Compared to existing results, the obtained CRB formulations have a different algebraic form with the help of some matrix equalities developed in this study. The new CRB expressions are helpful for obtaining some insights into the effects of various error sources on localization performance. Moreover, by comparing the CRBs for the four localization scenarios, some valuable insights are gained into the effects of various error sources on the estimation performance. Two kinds of location mean-square errors (MSE) expressions under the altitude constraint are deduced analytically using first-order error analysis and the Lagrange method. The first location MSE provides the theoretical prediction when an estimator assumes the satellite locations are precise but in fact have errors. The second location MSE provides the localization accuracy if an estimator assumes that the known calibration source locations are accurate while in fact erroneous. Then, the amount of reduction in localization accuracy due to the ignorance of satellite and calibration source location errors can be quantified. This allows us to decide whether the new algorithms to be accounted for satellite and calibration source position errors are necessary to improve the location accuracy. Also, the two location MSEs are compared to the corresponding CRBs. Although similar location MSEs have been deduced (Lu and Ho, 2006b; Ho et al., 2007; Ho and Yang, 2008; Yang and Ho, 2010b), the analyses did not involve an altitude

constraint, and consequently cannot be directly applied to satellite geolocation scenarios. In addition, these two location MSEs were not investigated by Ho and Chan (1997). Finally, simulations are provided to confirm the theoretical development.

## 2 Notations and preliminary results

### 2.1 Notations

In this paper, lowercase and uppercase boldface letters are used to denote vectors and matrices, respectively. In addition, the following conventions are used (Table 1).

**Table 1 Mathematical notation**

Notation	Explanation
$\text{diag}[\mathbf{a}]$	Diagonal matrix with diagonal entries formed from vector $\mathbf{a}$
$\text{blkdiag}[\mathbf{A}_1, \mathbf{A}_2]$	Block-diagonal matrix formed from matrices $\mathbf{A}_1$ and $\mathbf{A}_2$
$\text{Range}[\mathbf{A}]$	Linear subspace spanned by the column vectors of matrix $\mathbf{A}$
$\text{Rank}[\mathbf{A}]$	Dimension of the range-space of matrix $\mathbf{A}$
$\text{tr}(\mathbf{A})$	Trace of $\mathbf{A}$
$\mathbf{\Pi}(\mathbf{A})$	Orthogonal projection matrix onto the range-space of matrix $\mathbf{A}$
$\mathbf{\Pi}^\perp(\mathbf{A})$	Orthogonal projection matrix onto the null-space of matrix $\mathbf{A}^\top$
$\mathbf{O}_{n \times m}$	$n \times m$ matrix with all entries equal to zero
$\mathbf{I}_n$	$n \times n$ identity matrix
$E[\mathbf{A}]$	Covariance matrix

### 2.2 Preliminary results

In this section, some preliminary mathematical results used throughout this paper are developed.

**Theorem 1** Assume  $\mathbf{A}$  is an  $n \times n$  positive definite

matrix and  $\mathbf{b}$  is an  $n \times 1$  vector partitioned as  $\mathbf{b} = \begin{bmatrix} \bar{\mathbf{b}} \\ b_n \end{bmatrix}$ ,

where  $b_n$  is a nonzero scalar. Constructing an  $n \times (n-1)$

matrix related to  $\mathbf{b}$  as  $\Phi(\mathbf{b}) = \begin{bmatrix} \mathbf{I}_{n-1} \\ -\bar{\mathbf{b}}^\top / b_n \end{bmatrix}$ , it follows

that

$$\mathbf{A} - \frac{\mathbf{A}\mathbf{b}\mathbf{b}^\top\mathbf{A}}{\mathbf{b}^\top\mathbf{A}\mathbf{b}} = \Phi(\mathbf{b})(\Phi^\top(\mathbf{b})\mathbf{A}^{-1}\Phi(\mathbf{b}))^{-1}\Phi^\top(\mathbf{b}). \quad (1)$$

The proof of Theorem 1 is given in Appendix A. Based on Theorem 1, Theorem 2 can be obtained.

**Theorem 2** Assume  $A$  is an  $(n+m) \times (n+m)$  positive definite matrix and  $\mathbf{b}$  is an  $n$ -dimensional vector that can be partitioned as  $\mathbf{b} = \begin{bmatrix} \bar{\mathbf{b}} \\ b_n \end{bmatrix}$ , where  $b_n$  is a nonzero scalar. Constructing an  $n \times (n-1)$  matrix with  $\mathbf{b}$  as  $\Phi(\mathbf{b}) = \begin{bmatrix} \mathbf{I}_{n-1} \\ -\bar{\mathbf{b}}^T / b_n \end{bmatrix}$  and defining an  $(n+m) \times 1$  vector  $\mathbf{c} = [\mathbf{b}^T, \mathbf{O}_{1 \times m}]^T$ , which follows that

$$A - \frac{A\mathbf{c}\mathbf{c}^T A}{\mathbf{c}^T A \mathbf{c}} = \begin{bmatrix} \Phi(\mathbf{b}) & \mathbf{O}_{n \times m} \\ \mathbf{O}_{m \times (n-1)} & \mathbf{I}_m \end{bmatrix} \cdot \left( \begin{bmatrix} \Phi^T(\mathbf{b}) & \mathbf{O}_{(n-1) \times m} \\ \mathbf{O}_{m \times n} & \mathbf{I}_m \end{bmatrix} A^{-1} \begin{bmatrix} \Phi(\mathbf{b}) & \mathbf{O}_{n \times m} \\ \mathbf{O}_{m \times (n-1)} & \mathbf{I}_m \end{bmatrix} \right)^{-1} \cdot \begin{bmatrix} \Phi^T(\mathbf{b}) & \mathbf{O}_{(n-1) \times m} \\ \mathbf{O}_{m \times n} & \mathbf{I}_m \end{bmatrix} \quad (2)$$

The proof of Theorem 2 is provided in Appendix B. Note that with Theorems 1 and 2, we can obtain the CRB formulations in a new algebraic form, which differs from those of published formulations.

**Theorem 3** Assume  $A$  is an  $n \times n$  positive definite matrix and  $B$  is an  $n \times p$  matrix with a full column rank. Let  $C$  be an arbitrary  $n \times q$  matrix, we have

$$C^T A C - C^T A B (B^T A B)^{-1} B^T A^T C \geq \mathbf{O}. \quad (3)$$

The proof of Theorem 3 can be found in Ho and Yang (2008). Finally, two matrix inversion formulas used throughout this paper are listed in Table 2.

### 3 Measurement model and statistical assumptions

#### 3.1 Measurement model and statistical assumptions for an emitter signal

Consider a multi-satellite geolocation system with  $M$  satellites to locate a stationary emitter on the

surface of the Earth. To simplify the subsequent analysis, we choose an Earth-centered geosynchronous reference frame, and a Cartesian coordinate system with its  $z$  axis along the Earth's axis of rotation, and  $x$  and  $y$  axes in the equatorial plane. The true positions of the  $m$ th satellite and the emitter are denoted by  $\mathbf{s}_m^o$  and  $\mathbf{u}^o$ , respectively. For easy analysis, the emitter is assumed to be located at the Earth's surface with zero altitude at sea level. As a consequence, the position vector  $\mathbf{u}^o$  shall obey the following equation:

$$x^{u^o 2} + y^{u^o 2} + z^{u^o 2} / (1 - e^2) = r_e^2 \Leftrightarrow (\mathbf{u}^o)^T \mathbf{D} \mathbf{u}^o = r_e^2, \quad (4)$$

where  $\mathbf{u}^o = [x^{u^o}, y^{u^o}, z^{u^o}]^T$ ,  $r_e = 6378.137$  km is the equatorial radius,  $e = 0.08191908426214957$  is the first eccentricity, and  $\mathbf{D} = \text{diag}(1, 1, 1/(1 - e^2))$ . An observer on the Earth's surface receives the downlink signals radiated from the satellites, and the parameters used to determine the target position can be extracted from the received signals. The position of the ground observer is accurately known, denoted by  $\mathbf{r}^o$ . Without loss of generality, TDOA measurements are adopted for localization, and the theoretical analysis throughout this paper is based on this kind of measurement.

If the true TDOA of a signal retransmitted by the satellite pair  $m$  and 1 is  $\Delta t_{m1}^{u^o}$ , then the set of equations that relates the TDOAs and the source position is modeled as

$$\begin{aligned} \Delta t_{m1}^{u^o} &= h_m(\mathbf{u}^o, \mathbf{s}^o) \\ &= \frac{1}{c} (\|\mathbf{u}^o - \mathbf{s}_m^o\| + \|\mathbf{r}^o - \mathbf{s}_m^o\| \\ &\quad - \|\mathbf{u}^o - \mathbf{s}_1^o\| - \|\mathbf{r}^o - \mathbf{s}_1^o\|), \\ &2 \leq m \leq M, \end{aligned} \quad (5)$$

where  $c$  is the signal propagation speed, and  $\mathbf{s}^o = [\mathbf{s}_1^{oT}, \mathbf{s}_2^{oT}, \dots, \mathbf{s}_M^{oT}]^T$  includes all the position vectors of the satellites. For notation simplicity, we

Table 2 Matrix inversion formulas

No.	Matrix inversion formula
I	$\begin{bmatrix} A & B \\ C & D \end{bmatrix}^{-1} = \begin{bmatrix} (A - BD^{-1}C)^{-1} & -A^{-1}B(D - CA^{-1}B)^{-1} \\ -D^{-1}C(A - BD^{-1}C)^{-1} & (D - CA^{-1}B)^{-1} \end{bmatrix}$
II	$(A + BCD)^{-1} = A^{-1} - A^{-1}B(C^{-1} + DA^{-1}B)^{-1}DA^{-1}$

collect  $\Delta t_{m1}^{u0}$  and  $h_m(\mathbf{u}^0, \mathbf{s}^0)$  ( $2 \leq m \leq M$ ), respectively, to yield two  $(M-1) \times 1$  vectors as

$$\begin{cases} \Delta \mathbf{t}^{u0} = [\Delta t_{21}^{u0}, \Delta t_{31}^{u0}, \dots, \Delta t_{M1}^{u0}]^T, \\ \mathbf{h}(\mathbf{u}^0, \mathbf{s}^0) = [h_2(\mathbf{u}^0, \mathbf{s}^0), h_3(\mathbf{u}^0, \mathbf{s}^0), \dots, h_M(\mathbf{u}^0, \mathbf{s}^0)]^T. \end{cases} \quad (6)$$

From Eqs. (5) and (6),  $\Delta \mathbf{t}^{u0} = \mathbf{h}(\mathbf{u}^0, \mathbf{s}^0)$ .

If the ground observer can obtain the true TDOAs and the position information of the satellites are precisely determined, the emitter will be accurately located using Eqs. (4) and (5). Unfortunately, these ideal assumptions are not very realistic. In this study, we consider two kinds of errors that influence the localization accuracy. The first is TDOA estimation noise and the second is satellite position uncertainty.

Assume that the noisy versions of TDOAs from measurement are given by

$$\Delta t_{m1}^u = \Delta t_{m1}^{u0} + \Delta \tilde{t}_{m1}^u, \quad 2 \leq m \leq M, \quad (7)$$

where  $\Delta \tilde{t}_{m1}^u$  is the additive noise. Putting all the measurements and noises together yields two  $(M-1) \times 1$  vectors as

$$\begin{cases} \Delta \mathbf{t}^u = [\Delta t_{21}^u, \Delta t_{31}^u, \dots, \Delta t_{M1}^u]^T, \\ \Delta \tilde{\mathbf{t}}^u = [\Delta \tilde{t}_{21}^u, \Delta \tilde{t}_{31}^u, \dots, \Delta \tilde{t}_{M1}^u]^T. \end{cases} \quad (8)$$

From Eqs. (5)–(8) we deduce that

$$\Delta \mathbf{t}^u = \Delta \mathbf{t}^{u0} + \Delta \tilde{\mathbf{t}}^u = \mathbf{h}(\mathbf{u}^0, \mathbf{s}^0) + \Delta \tilde{\mathbf{t}}^u. \quad (9)$$

To simplify theoretical analysis,  $\Delta \tilde{\mathbf{t}}^u$  is modeled as a zero-mean Gaussian random process with a covariance matrix  $\mathbf{Q}_1 = E[\Delta \tilde{\mathbf{t}}^u \Delta \tilde{\mathbf{t}}^{uT}]$ .

Note that the precise satellite position may not be available in practice. In this situation, the perturbed satellite positions are modeled by

$$\mathbf{s}_m = \mathbf{s}_m^0 + \tilde{\mathbf{s}}_m, \quad 1 \leq m \leq M, \quad (10)$$

where  $\tilde{\mathbf{s}}_m$  is the measurement error. The collection of all the measurements and noises of the satellite position forms two  $3(M-1) \times 1$  vectors as

$$\begin{cases} \mathbf{s} = [\mathbf{s}_1^T, \mathbf{s}_2^T, \dots, \mathbf{s}_M^T]^T, \\ \tilde{\mathbf{s}} = [\tilde{\mathbf{s}}_1^T, \tilde{\mathbf{s}}_2^T, \dots, \tilde{\mathbf{s}}_M^T]^T. \end{cases} \quad (11)$$

From Eqs. (10) and (11), it follows that

$$\mathbf{s} = \mathbf{s}^0 + \tilde{\mathbf{s}}. \quad (12)$$

For mathematical convenience and motivated by the central limit theorem,  $\tilde{\mathbf{s}}$  is assumed to be Gaussian distributed with zero mean and covariance matrix  $\mathbf{Q}_2 = E[\tilde{\mathbf{s}} \tilde{\mathbf{s}}^T]$ .

### 3.2 Measurement model and statistical assumptions for calibration signals

To reduce the loss in localization accuracy due to the satellite position uncertainty, some calibration sources at known locations are usually deployed not far from the emitter. Suppose that a total of  $N$  calibration sources are used, and that the true position vector of the  $n$ th sources is denoted by  $\mathbf{v}_n^0$ . If the true TDOA associated with the  $n$ th calibration signal retransmitted by the satellite pair  $m$  and 1 is  $\Delta t_{nm1}^{v0}$ , then the set of equations that relates the TDOAs and the calibration source location can be directly obtained by replacing  $\mathbf{u}^0$  in Eq. (5) with  $\mathbf{v}_n^0$  as

$$\begin{aligned} \Delta t_{nm1}^{v0} &= h_m(\mathbf{v}_n^0, \mathbf{s}^0) \\ &= \frac{1}{c} (\|\mathbf{v}_n^0 - \mathbf{s}_m^0\| + \|\mathbf{r}^0 - \mathbf{s}_m^0\| \\ &\quad - \|\mathbf{v}_n^0 - \mathbf{s}_1^0\| - \|\mathbf{r}^0 - \mathbf{s}_1^0\|), \\ &1 \leq n \leq N \text{ and } 2 \leq m \leq M. \end{aligned} \quad (13)$$

Similarly, only the noisy version of  $\Delta t_{nm1}^{v0}$  is available in practice, modeled as

$$\Delta t_{nm1}^v = \Delta t_{nm1}^{v0} + \Delta \tilde{t}_{nm1}^v, \quad 1 \leq n \leq N, \quad 2 \leq m \leq M, \quad (14)$$

where  $\Delta \tilde{t}_{nm1}^v$  is the additive noise. For notation convenience, we collect  $\Delta t_{nm1}^v$ ,  $\Delta t_{nm1}^{v0}$ , and  $\Delta \tilde{t}_{nm1}^v$  ( $2 \leq m \leq M$ ), respectively, to form the following three  $(M-1) \times 1$  vectors:

$$\begin{cases} \Delta \mathbf{t}_n^v = [\Delta t_{n21}^v, \Delta t_{n31}^v, \dots, \Delta t_{nM1}^v]^T, \\ \Delta \mathbf{t}_n^{v0} = [\Delta t_{n21}^{v0}, \Delta t_{n31}^{v0}, \dots, \Delta t_{nM1}^{v0}]^T, \\ \Delta \tilde{\mathbf{t}}_n^v = [\Delta \tilde{t}_{n21}^v, \Delta \tilde{t}_{n31}^v, \dots, \Delta \tilde{t}_{nM1}^v]^T. \end{cases} \quad (15)$$

From Eqs. (13)–(15), it follows that

$$\Delta \mathbf{t}_n^v = \Delta \mathbf{t}_n^{v0} + \Delta \tilde{\mathbf{t}}_n^v = \mathbf{h}(\mathbf{v}_n^0, \mathbf{s}^0) + \Delta \tilde{\mathbf{t}}_n^v, \quad 1 \leq n \leq N. \quad (16)$$

Furthermore, the collections of  $\Delta \mathbf{t}_n^v$ ,  $\Delta \mathbf{t}_n^{v^0}$ , and  $\Delta \tilde{\mathbf{t}}_n^v$  ( $1 \leq n \leq M$ ), yield the following three  $(M-1)N \times 1$  vectors:

$$\begin{cases} \Delta \mathbf{t}^v = [\Delta \mathbf{t}_1^{vT}, \Delta \mathbf{t}_2^{vT}, \dots, \Delta \mathbf{t}_N^{vT}]^T, \\ \Delta \mathbf{t}^{v^0} = [\Delta \mathbf{t}_1^{v^0T}, \Delta \mathbf{t}_2^{v^0T}, \dots, \Delta \mathbf{t}_N^{v^0T}]^T, \\ \Delta \tilde{\mathbf{t}}^v = [\Delta \tilde{\mathbf{t}}_1^{vT}, \Delta \tilde{\mathbf{t}}_2^{vT}, \dots, \Delta \tilde{\mathbf{t}}_N^{vT}]^T. \end{cases} \quad (17)$$

Using Eqs. (16) and (17), we obtain

$$\Delta \mathbf{t}^v = \Delta \mathbf{t}^{v^0} + \Delta \tilde{\mathbf{t}}^v = \mathbf{g}(\mathbf{v}^0, \mathbf{s}^0) + \Delta \tilde{\mathbf{t}}^v, \quad (18)$$

where

$$\mathbf{g}(\mathbf{v}^0, \mathbf{s}^0) = [\mathbf{h}^T(\mathbf{v}_1^0, \mathbf{s}^0), \mathbf{h}^T(\mathbf{v}_2^0, \mathbf{s}^0), \dots, \mathbf{h}^T(\mathbf{v}_N^0, \mathbf{s}^0)]^T, \quad (19)$$

where  $\mathbf{v}^0 = [\mathbf{v}_1^{0T}, \mathbf{v}_2^{0T}, \dots, \mathbf{v}_N^{0T}]^T$  includes all the position vectors of the calibration sources. Analogously,  $\Delta \tilde{\mathbf{t}}^v$  is assumed to be Gaussian distributed with zero mean and covariance matrix  $\mathbf{P}_1 = E[\Delta \tilde{\mathbf{t}}^v \Delta \tilde{\mathbf{t}}^{vT}]$ .

In practice, the position measurements of the calibration emitters may also be corrupted by random errors. Assume that the noisy version of  $\mathbf{v}_n^0$  is given by

$$\mathbf{v}_n = \mathbf{v}_n^0 + \tilde{\mathbf{v}}_n, \quad 1 \leq n \leq N, \quad (20)$$

where  $\tilde{\mathbf{v}}_n$  is the measurement error vector. Since there are  $N$  calibration sources, the total position measurements and noises are

$$\begin{cases} \mathbf{v} = [\mathbf{v}_1^T, \mathbf{v}_2^T, \dots, \mathbf{v}_N^T]^T, \\ \tilde{\mathbf{v}} = [\tilde{\mathbf{v}}_1^T, \tilde{\mathbf{v}}_2^T, \dots, \tilde{\mathbf{v}}_N^T]^T. \end{cases} \quad (21)$$

It follows from Eqs. (20) and (21) that

$$\mathbf{v} = \mathbf{v}^0 + \tilde{\mathbf{v}}, \quad (22)$$

where  $\tilde{\mathbf{v}}$  is assumed to be Gaussian distributed with zeros mean and covariance matrix  $\mathbf{P}_2 = E[\tilde{\mathbf{v}}\tilde{\mathbf{v}}^T]$ .

#### 4 Analysis on the Cramér–Rao bound for multi-satellite joint geolocation

It is well known that the CRB establishes a lower bound on the error covariance matrix for any unbiased estimator, and is equal to the inverse of the Fisher information matrix (FIM) that is created from the

probability density function (PDF) of the underlying problem. This section is devoted to deriving the compact CRB expressions for multi-satellite joint geolocation. This differs from conventional CRB formulation (Ho and Yang, 2008; Yang and Ho, 2010b) in that the bounds developed here take the constraint of Eq. (4) into consideration. Also, although the constrained CRB was investigated by Ho and Chan (1997), the satellite position errors and calibration signals were not taken into account. As a consequence, the analysis and comparisons were not sufficiently comprehensive.

To gain more comprehensive insights, we derive the CRB formulations for four geolocation cases. In case (a), the satellite positions are assumed to be accurately known and, therefore, the use of calibration sources is not necessary. In case (b), the accurate satellite positions are not available but the calibration sources are not used. Consequently, the difference between the CRBs for cases (a) and (b) provides the amount of possible loss of accuracy resulting from satellite position errors. In case (c), the accurate satellite positions are not available and the calibration sources with an accurate knowledge of position are used. Then, through comparing the CRBs for cases (b) and (c), we can find the performance improvement due to the introduction of calibration sources at accurate positions. In case (d), neither the satellite positions nor the calibration source locations are precisely obtained. As a result, the amount of degradation in localization accuracy can be determined by comparing the CRBs for cases (c) and (d). Note that the obtained CRB formulations take an algebraic form different from that in Ho and Chan (1997). The new form is beneficial in providing insights into the effects of various error sources on localization performance.

##### 4.1 Case (a): in the absence of satellite position errors

Note that if accurate satellite positions are available, the adoption of calibration sources is not necessary. In this scenario, the measurement vector is  $\Delta \mathbf{t}^u$ , whose PDF  $\mathbf{u}^0$  is formulated as

$$p^{(a)}(\Delta \mathbf{t}^u; \mathbf{u}^0) = K^{(a)} \cdot \exp \left\{ -\frac{1}{2} (\Delta \mathbf{t}^u - \mathbf{h}(\mathbf{u}^0, \mathbf{s}^0))^T \mathbf{Q}_1^{-1} (\Delta \mathbf{t}^u - \mathbf{h}(\mathbf{u}^0, \mathbf{s}^0)) \right\}, \quad (23)$$

where  $K^{(a)}$  is a constant factor that does not depend on the unknowns. If there is no restriction on  $\mathbf{u}^0$ , the Fisher information matrix for  $\mathbf{u}^0$  can be written as

$$\mathbf{FISH}^{(a)}(\mathbf{u}^0) = \mathbf{H}_1^T(\mathbf{u}^0, \mathbf{s}^0) \mathbf{Q}_1^{-1} \mathbf{H}_1(\mathbf{u}^0, \mathbf{s}^0) = \mathbf{X}^{(a)}, \quad (24)$$

where  $H_1(\mathbf{u}^0, \mathbf{s}^0)$  is stated in Eq. (25) (see page 1367).

However, as stated in Section 3, vector  $\mathbf{u}^0$  must obey the constraint of Eq. (4). Consequently, the CRB matrix for  $\mathbf{u}^0$  is not simply the inverse of  $\mathbf{FISH}^{(a)}(\mathbf{u}^0)$ . According to the result in Marzetta (1993), the CRB matrix for  $\mathbf{u}^0$  under the constraint of Eq. (4) can be formulated as

$$\mathbf{CRB}^{(a)}(\mathbf{u}^0) = (\mathbf{X}^{(a)})^{-1} - \frac{(\mathbf{X}^{(a)})^{-1} \boldsymbol{\omega}^{(a)} \boldsymbol{\omega}^{(a)T} (\mathbf{X}^{(a)})^{-1}}{\boldsymbol{\omega}^{(a)T} (\mathbf{X}^{(a)})^{-1} \boldsymbol{\omega}^{(a)}}, \quad (26)$$

where

$$\boldsymbol{\omega}^{(a)} = [x^{u0}, y^{u0}, z^{u0} / (1 - e^2)]^T = \mathbf{D}\mathbf{u}^0. \quad (27)$$

Note that the second term on the right-hand side of Eq. (26) quantifies the improvement in localization accuracy resulting from incorporating the prior knowledge of  $\mathbf{u}^0$ .

According to Theorem 1,  $\mathbf{CRB}^{(a)}(\mathbf{u}^0)$  can be rephrased by

$$\mathbf{CRB}^{(a)}(\mathbf{u}^0) = \boldsymbol{\Phi}(\mathbf{D}\mathbf{u}^0) (\boldsymbol{\Phi}^T(\mathbf{D}\mathbf{u}^0) \mathbf{X}^{(a)} \boldsymbol{\Phi}(\mathbf{D}\mathbf{u}^0))^{-1} \cdot \boldsymbol{\Phi}^T(\mathbf{D}\mathbf{u}^0), \quad (28)$$

where

$$\boldsymbol{\Phi}(\mathbf{D}\mathbf{u}^0) = \left[ \begin{array}{c} \mathbf{I}_2 \\ \hline -(1 - e^2)x^{u0} / z^{u0} \quad | \quad -(1 - e^2)y^{u0} / z^{u0} \end{array} \right], \quad (29)$$

which is constructed in the manner described in Theorem 1. Obviously, the CRB formulation in Eq. (28) takes a different algebraic form from that of Eq. (26). The CRB expression in Eq. (28) is useful for subsequent analysis and comparison.

#### 4.2 Case (b): in the presence of satellite position errors and the absence of calibration sources

In this scenario, the measurements include both  $\Delta \mathbf{r}^u$  and  $\mathbf{s}$ , and the joint PDF of  $\Delta \mathbf{r}^u$  and  $\mathbf{s}$  parameterized on the unknowns  $\mathbf{u}^0$  and  $\mathbf{s}^0$  can be written as

$$p^{(b)}(\Delta \mathbf{r}^u, \mathbf{s}; \mathbf{u}^0, \mathbf{s}^0) = K^{(b)} \exp \left\{ -\frac{1}{2} (\Delta \mathbf{r}^u - \mathbf{h}(\mathbf{u}^0, \mathbf{s}^0))^T \cdot \mathbf{Q}_1^{-1} (\Delta \mathbf{r}^u - \mathbf{h}(\mathbf{u}^0, \mathbf{s}^0)) \right\} \cdot \exp \left\{ -\frac{1}{2} (\mathbf{s} - \mathbf{s}^0)^T \mathbf{Q}_2^{-1} (\mathbf{s} - \mathbf{s}^0) \right\}, \quad (30)$$

where  $K^{(b)}$  is a constant factor. If the constraint of Eq. (4) is ignored, the Fisher information matrix is given by

$$\mathbf{FISH}^{(b)} \left( \begin{bmatrix} \mathbf{u}^0 \\ \mathbf{s}^0 \end{bmatrix} \right) = \begin{bmatrix} \mathbf{X}^{(b)} & \mathbf{Y}^{(b)} \\ \mathbf{Y}^{(b)T} & \mathbf{Z}^{(b)} \end{bmatrix}, \quad (31)$$

where

$$\begin{cases} \mathbf{X}^{(b)} = \mathbf{H}_1^T(\mathbf{u}^0, \mathbf{s}^0) \mathbf{Q}_1^{-1} \mathbf{H}_1(\mathbf{u}^0, \mathbf{s}^0), \\ \mathbf{Y}^{(b)} = \mathbf{H}_1^T(\mathbf{u}^0, \mathbf{s}^0) \mathbf{Q}_1^{-1} \mathbf{H}_2(\mathbf{u}^0, \mathbf{s}^0), \\ \mathbf{Z}^{(b)} = \mathbf{H}_2^T(\mathbf{u}^0, \mathbf{s}^0) \mathbf{Q}_1^{-1} \mathbf{H}_2(\mathbf{u}^0, \mathbf{s}^0) + \mathbf{Q}_2^{-1}, \end{cases} \quad (32)$$

where  $H_2(\mathbf{u}^0, \mathbf{s}^0)$  is stated in Eq. (33) (see page 1367).

In general,  $\mathbf{H}_2(\mathbf{u}^0, \mathbf{s}^0)$  has a full row rank. Similarly, the CRB matrix is not simply the inverse of  $\mathbf{FISH}^{(b)}([\mathbf{u}^0, \mathbf{s}^0]^T)$  under the constraint of Eq. (4). Making use of the result in Marzetta (1993) again leads to

$$\mathbf{CRB}^{(b)} \left( \begin{bmatrix} \mathbf{u}^0 \\ \mathbf{s}^0 \end{bmatrix} \right) = \frac{\begin{bmatrix} \mathbf{X}^{(b)} & \mathbf{Y}^{(b)} \\ \mathbf{Y}^{(b)T} & \mathbf{Z}^{(b)} \end{bmatrix}^{-1} \boldsymbol{\omega}^{(b)} \boldsymbol{\omega}^{(b)T} \begin{bmatrix} \mathbf{X}^{(b)} & \mathbf{Y}^{(b)} \\ \mathbf{Y}^{(b)T} & \mathbf{Z}^{(b)} \end{bmatrix}^{-1}}{\boldsymbol{\omega}^{(b)T} \begin{bmatrix} \mathbf{X}^{(b)} & \mathbf{Y}^{(b)} \\ \mathbf{Y}^{(b)T} & \mathbf{Z}^{(b)} \end{bmatrix}^{-1} \boldsymbol{\omega}^{(b)}}, \quad (34)$$

where

$$\begin{aligned} \boldsymbol{\omega}^{(b)} &= [x^0, y^0, z^0 / (1 - e^2) \mid \mathbf{O}_{1 \times 3M}]^T \\ &= [\boldsymbol{\omega}^{(a)T} \mid \mathbf{O}_{1 \times 3M}]^T = [(\mathbf{D}\mathbf{u}^0)^T \mid \mathbf{O}_{1 \times 3M}]^T. \end{aligned} \quad (35)$$

With the application of Theorem 2,  $\mathbf{CRB}^{(b)}([\mathbf{u}^0, \mathbf{s}^0]^T)$  can be rewritten as

$$\begin{aligned}
 H_1(\mathbf{u}^0, \mathbf{s}^0) &= \frac{\partial \mathbf{h}(\mathbf{u}^0, \mathbf{s}^0)}{\partial \mathbf{u}^{0T}} \\
 &= \frac{1}{c} \left[ \frac{\mathbf{u}^0 - \mathbf{s}_2^0}{\|\mathbf{u}^0 - \mathbf{s}_2^0\|} - \frac{\mathbf{u}^0 - \mathbf{s}_1^0}{\|\mathbf{u}^0 - \mathbf{s}_1^0\|}, \frac{\mathbf{u}^0 - \mathbf{s}_3^0}{\|\mathbf{u}^0 - \mathbf{s}_3^0\|} - \frac{\mathbf{u}^0 - \mathbf{s}_1^0}{\|\mathbf{u}^0 - \mathbf{s}_1^0\|}, \dots, \frac{\mathbf{u}^0 - \mathbf{s}_M^0}{\|\mathbf{u}^0 - \mathbf{s}_M^0\|} - \frac{\mathbf{u}^0 - \mathbf{s}_1^0}{\|\mathbf{u}^0 - \mathbf{s}_1^0\|} \right]^T.
 \end{aligned} \tag{25}$$

$$\begin{aligned}
 H_2(\mathbf{u}^0, \mathbf{s}^0) &= \frac{\partial \mathbf{h}(\mathbf{u}^0, \mathbf{s}^0)}{\partial \mathbf{s}^{0T}} \\
 &= \frac{1}{c} \left[ \begin{array}{c|c|c|c} \frac{\mathbf{u}^0 - \mathbf{s}_1^0}{\|\mathbf{u}^0 - \mathbf{s}_1^0\|} + \frac{\mathbf{r}^0 - \mathbf{s}_1^0}{\|\mathbf{r}^0 - \mathbf{s}_1^0\|} & \frac{\mathbf{u}^0 - \mathbf{s}_1^0}{\|\mathbf{u}^0 - \mathbf{s}_1^0\|} + \frac{\mathbf{r}^0 - \mathbf{s}_1^0}{\|\mathbf{r}^0 - \mathbf{s}_1^0\|} & \dots & \frac{\mathbf{u}^0 - \mathbf{s}_1^0}{\|\mathbf{u}^0 - \mathbf{s}_1^0\|} + \frac{\mathbf{r}^0 - \mathbf{s}_1^0}{\|\mathbf{r}^0 - \mathbf{s}_1^0\|} \\ \hline \frac{\mathbf{s}_2^0 - \mathbf{u}^0}{\|\mathbf{u}^0 - \mathbf{s}_2^0\|} + \frac{\mathbf{s}_2^0 - \mathbf{r}^0}{\|\mathbf{r}^0 - \mathbf{s}_2^0\|} & \mathbf{O}_{3 \times 1} & \dots & \mathbf{O}_{3 \times 1} \\ \hline \mathbf{O}_{3 \times 1} & \frac{\mathbf{s}_3^0 - \mathbf{u}^0}{\|\mathbf{u}^0 - \mathbf{s}_3^0\|} + \frac{\mathbf{s}_3^0 - \mathbf{r}^0}{\|\mathbf{r}^0 - \mathbf{s}_3^0\|} & \ddots & \vdots \\ \hline \vdots & \vdots & \ddots & \mathbf{O}_{3 \times 1} \\ \hline \mathbf{O}_{3 \times 1} & \dots & \mathbf{O}_{3 \times 1} & \frac{\mathbf{s}_M^0 - \mathbf{u}^0}{\|\mathbf{u}^0 - \mathbf{s}_M^0\|} + \frac{\mathbf{s}_M^0 - \mathbf{r}^0}{\|\mathbf{r}^0 - \mathbf{s}_M^0\|} \end{array} \right]^T.
 \end{aligned} \tag{33}$$

$$\begin{aligned}
 \text{CRB}^{(b)} \left( \begin{bmatrix} \mathbf{u}^0 \\ \mathbf{s}^0 \end{bmatrix} \right) &= \begin{bmatrix} \Phi(\mathbf{D}\mathbf{u}^0) & \mathbf{O}_{3 \times 3M} \\ \mathbf{O}_{3M \times 2} & \mathbf{I}_{3M} \end{bmatrix} \\
 &\cdot \left( \begin{bmatrix} \Phi^T(\mathbf{D}\mathbf{u}^0) & \mathbf{O}_{2 \times 3M} \\ \mathbf{O}_{3M \times 3} & \mathbf{I}_{3M} \end{bmatrix} \begin{bmatrix} \mathbf{X}^{(b)} & \mathbf{Y}^{(b)} \\ \mathbf{Y}^{(b)T} & \mathbf{Z}^{(b)} \end{bmatrix} \right) \\
 &\cdot \left( \begin{bmatrix} \Phi(\mathbf{D}\mathbf{u}^0) & \mathbf{O}_{3 \times 3M} \\ \mathbf{O}_{3M \times 2} & \mathbf{I}_{3M} \end{bmatrix} \right)^{-1} \\
 &\cdot \begin{bmatrix} \Phi^T(\mathbf{D}\mathbf{u}^0) & \mathbf{O}_{2 \times 3M} \\ \mathbf{O}_{3M \times 3} & \mathbf{I}_{3M} \end{bmatrix}.
 \end{aligned} \tag{36}$$

Furthermore, the use of matrix inversion formulas in Table 2 yields

$$\begin{aligned}
 \text{CRB}^{(b)}(\mathbf{u}^0) &= \Phi(\mathbf{D}\mathbf{u}^0) [\Phi^T(\mathbf{D}\mathbf{u}^0) (\mathbf{X}^{(b)} - \mathbf{Y}^{(b)} (\mathbf{Z}^{(b)})^{-1} \mathbf{Y}^{(b)T}) \Phi(\mathbf{D}\mathbf{u}^0)]^{-1} \\
 &\cdot \Phi^T(\mathbf{D}\mathbf{u}^0) \\
 &= \Phi(\mathbf{D}\mathbf{u}^0) (\Phi^T(\mathbf{D}\mathbf{u}^0) \mathbf{X}^{(b)} \Phi(\mathbf{D}\mathbf{u}^0))^{-1} \Phi^T(\mathbf{D}\mathbf{u}^0) \\
 &+ \Phi(\mathbf{D}\mathbf{u}^0) (\Phi^T(\mathbf{D}\mathbf{u}^0) \mathbf{X}^{(b)} \Phi(\mathbf{D}\mathbf{u}^0))^{-1} \\
 &\cdot \Phi^T(\mathbf{D}\mathbf{u}^0) \mathbf{Y}^{(b)} [\mathbf{Z}^{(b)} - \mathbf{Y}^{(b)T} \Phi(\mathbf{D}\mathbf{u}^0)]^{-1} \\
 &\cdot (\Phi^T(\mathbf{D}\mathbf{u}^0) \mathbf{X}^{(b)} \Phi(\mathbf{D}\mathbf{u}^0))^{-1} \Phi^T(\mathbf{D}\mathbf{u}^0) \mathbf{Y}^{(b)} ]^{-1} \\
 &\cdot \mathbf{Y}^{(b)T} \Phi(\mathbf{D}\mathbf{u}^0) (\Phi^T(\mathbf{D}\mathbf{u}^0) \mathbf{X}^{(b)} \Phi(\mathbf{D}\mathbf{u}^0))^{-1} \Phi^T(\mathbf{D}\mathbf{u}^0),
 \end{aligned} \tag{37}$$

$$\begin{aligned}
 \text{CRB}^{(b)}(\mathbf{s}^0) &= [\mathbf{Z}^{(b)} - \mathbf{Y}^{(b)T} \Phi(\mathbf{D}\mathbf{u}^0) (\Phi^T(\mathbf{D}\mathbf{u}^0) \mathbf{X}^{(b)} \Phi(\mathbf{D}\mathbf{u}^0))^{-1} \\
 &\cdot \Phi^T(\mathbf{D}\mathbf{u}^0) \mathbf{Y}^{(b)} ]^{-1} \\
 &= (\mathbf{Z}^{(b)})^{-1} + (\mathbf{Z}^{(b)})^{-1} \mathbf{Y}^{(b)T} \Phi(\mathbf{D}\mathbf{u}^0) \\
 &\cdot [\Phi^T(\mathbf{D}\mathbf{u}^0) (\mathbf{X}^{(b)} - \mathbf{Y}^{(b)} (\mathbf{Z}^{(b)})^{-1} \mathbf{Y}^{(b)T}) \Phi(\mathbf{D}\mathbf{u}^0)]^{-1} \\
 &\cdot \Phi^T(\mathbf{D}\mathbf{u}^0) \mathbf{Y}^{(b)} (\mathbf{Z}^{(b)})^{-1}.
 \end{aligned} \tag{38}$$

Combining Eqs. (28), (37), and (38), some important results can be drawn in the sequel, which we state formally as Propositions 1–3.

**Proposition 1**  $\text{CRB}^{(b)}(\mathbf{u}^0) \geq \text{CRB}^{(a)}(\mathbf{u}^0)$ .

Proposition 1 is proved in Appendix C. Proposition 1 indicates an obvious fact that satellite position uncertainty may cause degradation in emitter location precision.

**Proposition 2** Define the matrix

$$\tilde{\mathbf{Q}}_1 = \mathbf{Q}_1 + \mathbf{H}_2(\mathbf{u}^0, \mathbf{s}^0) \mathbf{Q}_2 \mathbf{H}_2^T(\mathbf{u}^0, \mathbf{s}^0). \tag{39}$$

Then,  $\text{CRB}^{(b)}(\mathbf{u}^0)$  can be represented by

$$\begin{aligned}
 \text{CRB}^{(b)}(\mathbf{u}^0) &= \Phi(\mathbf{D}\mathbf{u}^0) \\
 &\cdot (\Phi^T(\mathbf{D}\mathbf{u}^0) \mathbf{H}_1^T(\mathbf{u}^0, \mathbf{s}^0) \tilde{\mathbf{Q}}_1^{-1} \mathbf{H}_1(\mathbf{u}^0, \mathbf{s}^0) \Phi(\mathbf{D}\mathbf{u}^0))^{-1} \\
 &\cdot \Phi^T(\mathbf{D}\mathbf{u}^0).
 \end{aligned} \tag{40}$$

The proof of Proposition 2 is given in Appendix D. Proposition 2 states that  $\text{CRB}^{(b)}(\mathbf{u}^0)$  can be



considered as the CRB of an equivalent localization problem where the accurate satellite positions are available but the TDOA measurements are degraded to have an increased covariance matrix of  $\mathbf{Q}_1 + \mathbf{H}_2(\mathbf{u}^0, \mathbf{s}^0)\mathbf{Q}_2\mathbf{H}_2^T(\mathbf{u}^0, \mathbf{s}^0)$ . This observation leads to an interesting interpretation that the satellite position errors affect the emitter localization precision through increasing TDOA measurement errors.

**Proposition 3** If  $M=3$ , then  $\text{CRB}^{(b)}(\mathbf{s}^0) = \mathbf{Q}_2$ ; if  $M>3$ , then  $\text{CRB}^{(b)}(\mathbf{s}^0) < \mathbf{Q}_2$ .

Proposition 3 is proved in Appendix E. Proposition 3 reveals that if we want to obtain a lower estimation variance for satellite position from TDOA measurements, the location problem requires at least four satellites to produce three TDOAs.

### 4.3 Case (c): in the presence of calibration sources at accurate locations

In this scenario, the measurements include  $\Delta\mathbf{t}^u$ ,  $\Delta\mathbf{t}^v$ , and  $\mathbf{s}$ , and the joint PDF of  $\Delta\mathbf{t}^u$ ,  $\Delta\mathbf{t}^v$ , and  $\mathbf{s}$  parameterized on the unknowns  $\mathbf{u}^0$  and  $\mathbf{s}^0$  can be written as

$$p^{(c)}(\Delta\mathbf{t}^u, \Delta\mathbf{t}^v, \mathbf{s}; \mathbf{u}^0, \mathbf{s}^0) = K^{(c)} \cdot \exp\left\{-\frac{1}{2}(\Delta\mathbf{t}^u - \mathbf{h}(\mathbf{u}^0, \mathbf{s}^0))^T \mathbf{Q}_1^{-1}(\Delta\mathbf{t}^u - \mathbf{h}(\mathbf{u}^0, \mathbf{s}^0))\right\} \cdot \exp\left\{-\frac{1}{2}(\mathbf{s} - \mathbf{s}^0)^T \mathbf{Q}_2^{-1}(\mathbf{s} - \mathbf{s}^0)\right\} \cdot \exp\left\{-\frac{1}{2}(\Delta\mathbf{t}^v - \mathbf{g}(\mathbf{v}^0, \mathbf{s}^0))^T \mathbf{P}_1^{-1}(\Delta\mathbf{t}^v - \mathbf{g}(\mathbf{v}^0, \mathbf{s}^0))\right\}, \quad (41)$$

where  $K^{(c)}$  is a constant factor. Similar to case (b), if the constraint of Eq. (4) is not considered, the Fisher information matrix is given by

$$\text{FISH}^{(c)}\left(\begin{bmatrix} \mathbf{u}^0 \\ \mathbf{s}^0 \end{bmatrix}\right) = \begin{bmatrix} \mathbf{X}^{(c)} & \mathbf{Y}^{(c)} \\ \mathbf{Y}^{(c)T} & \mathbf{Z}^{(c)} \end{bmatrix}, \quad (42)$$

where

$$\begin{cases} \mathbf{X}^{(c)} = \mathbf{H}_1^T(\mathbf{u}^0, \mathbf{s}^0)\mathbf{Q}_1^{-1}\mathbf{H}_1(\mathbf{u}^0, \mathbf{s}^0), \\ \mathbf{Y}^{(c)} = \mathbf{H}_1^T(\mathbf{u}^0, \mathbf{s}^0)\mathbf{Q}_1^{-1}\mathbf{H}_2(\mathbf{u}^0, \mathbf{s}^0), \\ \mathbf{Z}^{(c)} = \mathbf{H}_2^T(\mathbf{u}^0, \mathbf{s}^0)\mathbf{Q}_1^{-1}\mathbf{H}_2(\mathbf{u}^0, \mathbf{s}^0) + \mathbf{Q}_2^{-1} \\ \quad + \mathbf{G}_2^T(\mathbf{v}^0, \mathbf{s}^0)\mathbf{P}_1^{-1}\mathbf{G}_2(\mathbf{v}^0, \mathbf{s}^0), \end{cases} \quad (43)$$

where

$$\mathbf{G}_2(\mathbf{v}^0, \mathbf{s}^0) = \frac{\partial \mathbf{g}(\mathbf{v}^0, \mathbf{s}^0)}{\partial \mathbf{s}^{0T}} = [\mathbf{H}_2^T(\mathbf{v}_1^0, \mathbf{s}^0), \mathbf{H}_2^T(\mathbf{v}_2^0, \mathbf{s}^0), \dots, \mathbf{H}_2^T(\mathbf{v}_N^0, \mathbf{s}^0)]^T. \quad (44)$$

Analogously, the CRB matrix is not equal to the inverse of  $\text{FISH}^{(c)}([\mathbf{u}^0, \mathbf{s}^0]^T)$  under the constraint of Eq. (4). Applying the result in Marzetta (1993), the CRB matrix is formulated as

$$\text{CRB}^{(c)}\left(\begin{bmatrix} \mathbf{u}^0 \\ \mathbf{s}^0 \end{bmatrix}\right) = \frac{\begin{bmatrix} \mathbf{X}^{(c)} & \mathbf{Y}^{(c)} \\ \mathbf{Y}^{(c)T} & \mathbf{Z}^{(c)} \end{bmatrix}^{-1} \boldsymbol{\omega}^{(c)} \boldsymbol{\omega}^{(c)T} \begin{bmatrix} \mathbf{X}^{(c)} & \mathbf{Y}^{(c)} \\ \mathbf{Y}^{(c)T} & \mathbf{Z}^{(c)} \end{bmatrix}^{-1}}{\boldsymbol{\omega}^{(c)T} \begin{bmatrix} \mathbf{X}^{(c)} & \mathbf{Y}^{(c)} \\ \mathbf{Y}^{(c)T} & \mathbf{Z}^{(c)} \end{bmatrix}^{-1} \boldsymbol{\omega}^{(c)}}, \quad (45)$$

where

$$\boldsymbol{\omega}^{(c)} = \boldsymbol{\omega}^{(b)} = [x^0 \ y^0 \ z^0 / (1 - e^2) \mid \mathbf{O}_{1 \times 3M}]^T = [(\mathbf{D}\mathbf{u}^0)^T \mid \mathbf{O}_{1 \times 3M}]^T. \quad (46)$$

In addition, using the result in Theorem 2,  $\text{CRB}^{(c)}([\mathbf{u}^0, \mathbf{s}^0]^T)$  can be represented as

$$\text{CRB}^{(c)}\left(\begin{bmatrix} \mathbf{u}^0 \\ \mathbf{s}^0 \end{bmatrix}\right) = \begin{bmatrix} \boldsymbol{\Phi}(\mathbf{D}\mathbf{u}^0) & \mathbf{O}_{3 \times 3M} \\ \mathbf{O}_{3M \times 2} & \mathbf{I}_{3M} \end{bmatrix} \cdot \left( \begin{bmatrix} \boldsymbol{\Phi}^T(\mathbf{D}\mathbf{u}^0) & \mathbf{O}_{2 \times 3M} \\ \mathbf{O}_{3M \times 3} & \mathbf{I}_{3M} \end{bmatrix} \begin{bmatrix} \mathbf{X}^{(c)} & \mathbf{Y}^{(c)} \\ \mathbf{Y}^{(c)T} & \mathbf{Z}^{(c)} \end{bmatrix} \right)^{-1} \cdot \begin{bmatrix} \boldsymbol{\Phi}^T(\mathbf{D}\mathbf{u}^0) & \mathbf{O}_{2 \times 3M} \\ \mathbf{O}_{3M \times 3} & \mathbf{I}_{3M} \end{bmatrix}. \quad (47)$$

Employing the matrix inversion formulas in Table 2 again, we arrive at

$$\begin{aligned} \text{CRB}^{(c)}(\mathbf{u}^0) &= \boldsymbol{\Phi}(\mathbf{D}\mathbf{u}^0)[\boldsymbol{\Phi}^T(\mathbf{D}\mathbf{u}^0) \\ &\cdot (\mathbf{X}^{(c)} - \mathbf{Y}^{(c)}(\mathbf{Z}^{(c)})^{-1}\mathbf{Y}^{(c)T})\boldsymbol{\Phi}(\mathbf{D}\mathbf{u}^0)]^{-1}\boldsymbol{\Phi}^T(\mathbf{D}\mathbf{u}^0) \\ &= \boldsymbol{\Phi}(\mathbf{D}\mathbf{u}^0)(\boldsymbol{\Phi}^T(\mathbf{D}\mathbf{u}^0)\mathbf{X}^{(c)}\boldsymbol{\Phi}(\mathbf{D}\mathbf{u}^0))^{-1}\boldsymbol{\Phi}^T(\mathbf{D}\mathbf{u}^0) \\ &\quad + \boldsymbol{\Phi}(\mathbf{D}\mathbf{u}^0)(\boldsymbol{\Phi}^T(\mathbf{D}\mathbf{u}^0)\mathbf{X}^{(c)}\boldsymbol{\Phi}(\mathbf{D}\mathbf{u}^0))^{-1} \\ &\quad \cdot \boldsymbol{\Phi}^T(\mathbf{D}\mathbf{u}^0)\mathbf{Y}^{(c)}(\mathbf{Z}^{(c)} - \mathbf{Y}^{(c)T}\boldsymbol{\Phi}(\mathbf{D}\mathbf{u}^0))^{-1} \\ &\quad \cdot (\boldsymbol{\Phi}^T(\mathbf{D}\mathbf{u}^0)\mathbf{X}^{(c)}\boldsymbol{\Phi}(\mathbf{D}\mathbf{u}^0))^{-1}\boldsymbol{\Phi}^T(\mathbf{D}\mathbf{u}^0)\mathbf{Y}^{(c)} \\ &\quad \cdot \boldsymbol{\Phi}(\mathbf{D}\mathbf{u}^0)(\boldsymbol{\Phi}^T(\mathbf{D}\mathbf{u}^0)\mathbf{X}^{(c)}\boldsymbol{\Phi}(\mathbf{D}\mathbf{u}^0))^{-1}\boldsymbol{\Phi}^T(\mathbf{D}\mathbf{u}^0), \end{aligned} \quad (48)$$

$$\begin{aligned} \text{CRB}^{(c)}(\mathbf{s}^o) &= [\mathbf{Z}^{(c)} - \mathbf{Y}^{(c)\text{T}} \boldsymbol{\Phi}(\mathbf{D}\mathbf{u}^o)(\boldsymbol{\Phi}^{\text{T}}(\mathbf{D}\mathbf{u}^o) \\ &\quad \cdot \mathbf{X}^{(c)} \boldsymbol{\Phi}(\mathbf{D}\mathbf{u}^o))^{-1} \boldsymbol{\Phi}^{\text{T}}(\mathbf{D}\mathbf{u}^o) \mathbf{Y}^{(c)}]^{-1} \\ &= (\mathbf{Z}^{(c)})^{-1} + (\mathbf{Z}^{(c)})^{-1} \mathbf{Y}^{(c)\text{T}} \boldsymbol{\Phi}(\mathbf{D}\mathbf{u}^o) \\ &\quad \cdot [\boldsymbol{\Phi}^{\text{T}}(\mathbf{D}\mathbf{u}^o)(\mathbf{X}^{(c)} - \mathbf{Y}^{(c)}(\mathbf{Z}^{(c)})^{-1} \mathbf{Y}^{(c)\text{T}}) \\ &\quad \cdot \boldsymbol{\Phi}(\mathbf{D}\mathbf{u}^o)]^{-1} \boldsymbol{\Phi}^{\text{T}}(\mathbf{D}\mathbf{u}^o) \mathbf{Y}^{(c)} (\mathbf{Z}^{(c)})^{-1}. \end{aligned} \quad (49)$$

Combining Eqs. (28), (37), (38), (48), and (49), some important results can be concluded in the sequel, which we state formally as Propositions 4–6.

**Proposition 4**  $\text{CRB}^{(b)}(\mathbf{u}^o) \geq \text{CRB}^{(c)}(\mathbf{u}^o) \geq \text{CRB}^{(a)}(\mathbf{u}^o)$ .

The proof of Proposition 4 can be found in Appendix F. Proposition 4 indicates that it is beneficial to use the calibration sources at accurate locations to increase the best localization accuracy when satellites position errors are present. However, it is hard to achieve the best localization precision in the absence of satellite position uncertainty. However, under certain ideal conditions, it is possible to completely eliminate the effects of satellite position errors on emitter localization precision. This conclusion is supported by Proposition 5.

**Proposition 5** If  $\mathbf{G}_2(\mathbf{v}^o, \mathbf{s}^o)$  has a full column rank, then it follows that  $\lim_{P_1 \rightarrow 0} \text{CRB}^{(c)}(\mathbf{u}^o) = \text{CRB}^{(a)}(\mathbf{u}^o)$ .

Proposition 5 is proved in Appendix G. An intuitive explanation of Proposition 5 is that when the calibration TDOAs are noiseless and  $\mathbf{G}_2(\mathbf{v}^o, \mathbf{s}^o)$  is a full-column rank matrix, the  $3M \times 1$  satellite position vector  $\mathbf{s}^o$  can be uniquely identified using the TDOA Eq. (13). As a consequence, the emitter location accuracy becomes unaffected by the satellite position errors. In addition, the full-column rank property of  $\mathbf{G}_2(\mathbf{v}^o, \mathbf{s}^o)$  leads to  $(M-1)N \geq 3M$ , which means that  $N \geq 4$ , i.e., at least four calibration sources are needed.

**Proposition 6**  $\text{CRB}^{(c)}(\mathbf{s}^o) \leq \text{CRB}^{(b)}(\mathbf{s}^o)$ , and if  $\mathbf{G}_2(\mathbf{v}^o, \mathbf{s}^o)$  has full column rank, then  $\text{CRB}^{(c)}(\mathbf{s}^o) < \text{CRB}^{(b)}(\mathbf{s}^o)$ .

The proof of Proposition 6 is straightforward, and it is omitted here due to limited space. Proposition 6 demonstrates that the calibration TDOAs can be used to improve the best achievable estimation accuracy for satellite position in case (b).

#### 4.4 Case (d): in the presence of calibration sources at inaccurate locations

If the position of the calibration sources cannot be accurately obtained, the vector  $\mathbf{v}^o$  shall be viewed

as the unknowns. In this scenario, the measurements include  $\Delta \mathbf{t}^u, \Delta \mathbf{t}^v, \mathbf{s}$ , and  $\mathbf{v}$ , and the joint PDF of  $\Delta \mathbf{t}^u, \Delta \mathbf{t}^v, \mathbf{s}$ , and  $\mathbf{v}$  parameterized on the unknowns  $\mathbf{u}^o, \mathbf{s}^o$ , and  $\mathbf{v}^o$  can be written as

$$\begin{aligned} p^{(d)}(\Delta \mathbf{t}^u, \Delta \mathbf{t}^v, \mathbf{s}, \mathbf{v}; \mathbf{u}^o, \mathbf{s}^o, \mathbf{v}^o) &= K^{(d)} \\ &\cdot \exp \left\{ -\frac{1}{2} (\Delta \mathbf{t}^u - \mathbf{h}(\mathbf{u}^o, \mathbf{s}^o))^{\text{T}} \mathbf{Q}_1^{-1} (\Delta \mathbf{t}^u - \mathbf{h}(\mathbf{u}^o, \mathbf{s}^o)) \right\} \\ &\cdot \exp \left\{ -\frac{1}{2} (\mathbf{s} - \mathbf{s}^o)^{\text{T}} \mathbf{Q}_2^{-1} (\mathbf{s} - \mathbf{s}^o) \right\} \\ &\cdot \exp \left\{ -\frac{1}{2} (\Delta \mathbf{t}^v - \mathbf{g}(\mathbf{v}^o, \mathbf{s}^o))^{\text{T}} \mathbf{P}_1^{-1} (\Delta \mathbf{t}^v - \mathbf{g}(\mathbf{v}^o, \mathbf{s}^o)) \right\} \\ &\cdot \exp \left\{ -\frac{1}{2} (\mathbf{v} - \mathbf{v}^o)^{\text{T}} \mathbf{P}_2^{-1} (\mathbf{v} - \mathbf{v}^o) \right\}, \end{aligned} \quad (50)$$

where  $K^{(b)}$  is a constant factor. If the constraint of Eq. (4) is neglected, the Fisher information matrix is given by

$$\text{FISH}^{(d)} \begin{pmatrix} \mathbf{u}^o \\ \mathbf{s}^o \\ \mathbf{v}^o \end{pmatrix} = \begin{bmatrix} \mathbf{X}^{(d)} & \mathbf{Y}^{(d)} & \mathbf{O} \\ \mathbf{Y}^{(d)\text{T}} & \mathbf{Z}^{(d)} & \mathbf{W}^{(d)\text{T}} \\ \mathbf{O} & \mathbf{W}^{(d)} & \mathbf{T}^{(d)} \end{bmatrix}, \quad (51)$$

where

$$\begin{cases} \mathbf{X}^{(d)} = \mathbf{H}_1^{\text{T}}(\mathbf{u}^o, \mathbf{s}^o) \mathbf{Q}_1^{-1} \mathbf{H}_1(\mathbf{u}^o, \mathbf{s}^o), \\ \mathbf{Y}^{(d)} = \mathbf{H}_1^{\text{T}}(\mathbf{u}^o, \mathbf{s}^o) \mathbf{Q}_1^{-1} \mathbf{H}_2(\mathbf{u}^o, \mathbf{s}^o), \\ \mathbf{Z}^{(d)} = \mathbf{H}_2^{\text{T}}(\mathbf{u}^o, \mathbf{s}^o) \mathbf{Q}_1^{-1} \mathbf{H}_2(\mathbf{u}^o, \mathbf{s}^o) + \mathbf{Q}_2^{-1} \\ \quad + \mathbf{G}_2^{\text{T}}(\mathbf{v}^o, \mathbf{s}^o) \mathbf{P}_1^{-1} \mathbf{G}_2(\mathbf{v}^o, \mathbf{s}^o), \\ \mathbf{W}^{(d)} = \mathbf{G}_1^{\text{T}}(\mathbf{v}^o, \mathbf{s}^o) \mathbf{P}_1^{-1} \mathbf{G}_2(\mathbf{v}^o, \mathbf{s}^o), \\ \mathbf{T}^{(d)} = \mathbf{G}_1^{\text{T}}(\mathbf{v}^o, \mathbf{s}^o) \mathbf{P}_1^{-1} \mathbf{G}_1(\mathbf{v}^o, \mathbf{s}^o) + \mathbf{P}_2^{-1}, \end{cases} \quad (52)$$

where

$$\begin{aligned} \mathbf{G}_1(\mathbf{v}^o, \mathbf{s}^o) &= \frac{\partial \mathbf{g}(\mathbf{v}^o, \mathbf{s}^o)}{\partial \mathbf{v}^{o\text{T}}} \\ &= \text{blkdiag}[\mathbf{H}_1(\mathbf{v}_1^o, \mathbf{s}^o), \mathbf{H}_1(\mathbf{v}_2^o, \mathbf{s}^o), \dots, \mathbf{H}_1(\mathbf{v}_N^o, \mathbf{s}^o)]. \end{aligned} \quad (53)$$

Using the result in Marzetta (1993), the CRB matrix under the constraint of Eq. (4) is formulated as Eq. (54) (see page 1371), where

$$\begin{aligned} \boldsymbol{\omega}^{(d)} &= [x^o, y^o, z^o / (1 - e^2) \mid \mathbf{O}_{1 \times 3(M+N)}]^{\text{T}} \\ &= [(\mathbf{D}\mathbf{u}^o)^{\text{T}} \mid \mathbf{O}_{1 \times 3(M+N)}]^{\text{T}}. \end{aligned} \quad (54)$$

Once again, applying the result in Theorem 2, we can represent  $\mathbf{CRB}^{(d)}([\mathbf{u}^0, \mathbf{s}^0, \mathbf{v}^0]^T)$  as Eq. (56) (see page 1371).

Using the matrix inversion formulas in Table 2 yields Eqs. (57)–(59) (see page 1371).

Combining Eqs. (28), (37), (38), (48), (49), (57), (58), and (59), some important results can be obtained in the sequel, which we state formally as Propositions 7–10.

**Proposition 7**  $\mathbf{CRB}^{(b)}(\mathbf{u}^0) \geq \mathbf{CRB}^{(d)}(\mathbf{u}^0) \geq \mathbf{CRB}^{(c)}(\mathbf{u}^0) \geq \mathbf{CRB}^{(a)}(\mathbf{u}^0)$ .

The proof of Proposition 7 is provided in Appendix H. Proposition 7 indicates that the best achievable localization accuracy with calibration source position errors will be worse than one with accurate calibration position information. It also reveals that although their positions are not known exactly, using the calibration sources provides potential improvement in target localization accuracy.

**Proposition 8** Define a matrix

$$\tilde{\mathbf{P}}_1 = \mathbf{P}_1 + \mathbf{G}_1(\mathbf{v}^0, \mathbf{s}^0) \mathbf{P}_2 \mathbf{G}_1^T(\mathbf{v}^0, \mathbf{s}^0), \quad (60)$$

which can be used to form a novel matrix as follows:

$$\begin{aligned} \tilde{\mathbf{Z}}^{(c)} &= \mathbf{Z}^{(b)} + \mathbf{G}_2^T(\mathbf{v}^0, \mathbf{s}^0) \tilde{\mathbf{P}}_1^{-1} \mathbf{G}_2(\mathbf{v}^0, \mathbf{s}^0) \\ &= \mathbf{H}_2^T(\mathbf{u}^0, \mathbf{s}^0) \mathbf{Q}_1^{-1} \mathbf{H}_2(\mathbf{u}^0, \mathbf{s}^0) + \mathbf{Q}_2^{-1} \\ &\quad + \mathbf{G}_2^T(\mathbf{v}^0, \mathbf{s}^0) \tilde{\mathbf{P}}_1^{-1} \mathbf{G}_2(\mathbf{v}^0, \mathbf{s}^0). \end{aligned} \quad (61)$$

Then,  $\mathbf{CRB}^{(d)}(\mathbf{u}^0)$  can be represented by

$$\begin{aligned} \mathbf{CRB}^{(d)}(\mathbf{u}^0) &= \Phi(\mathbf{D}\mathbf{u}^0) \\ &\quad \cdot [\Phi^T(\mathbf{D}\mathbf{u}^0)(\mathbf{X}^{(c)} - \mathbf{Y}^{(c)}(\tilde{\mathbf{Z}}^{(c)})^{-1} \mathbf{Y}^{(c)T}) \\ &\quad \cdot \Phi(\mathbf{D}\mathbf{u}^0)]^{-1} \Phi^T(\mathbf{D}\mathbf{u}^0). \end{aligned} \quad (62)$$

Proposition 8 can be directly proved with Eq. (H5) in Appendix H. Proposition 8 indicates that  $\mathbf{CRB}^{(d)}(\mathbf{u}^0)$  can be considered as the CRB of an equivalent localization problem, where the accurate calibration source positions are available but the calibration TDOA measurements are degraded to have an increased covariance matrix of  $\mathbf{P}_1 + \mathbf{G}_1(\mathbf{v}^0, \mathbf{s}^0) \mathbf{P}_2 \mathbf{G}_1^T(\mathbf{v}^0, \mathbf{s}^0)$ . This observation leads to an interesting interpretation that the calibration source position errors affect the source localization accuracy through decreasing the quality of the calibration TDOA measurements.

**Proposition 9**  $\mathbf{CRB}^{(c)}(\mathbf{s}^0) \leq \mathbf{CRB}^{(d)}(\mathbf{s}^0) \leq \mathbf{CRB}^{(b)}(\mathbf{s}^0)$ ,

and if  $\mathbf{G}_2(\mathbf{v}^0, \mathbf{s}^0)$  has a full column rank, then  $\mathbf{CRB}^{(c)}(\mathbf{s}^0) < \mathbf{CRB}^{(d)}(\mathbf{s}^0) < \mathbf{CRB}^{(b)}(\mathbf{s}^0)$ .

The proof of Proposition 9 is straightforward, but it is omitted here due to limited space. Proposition 9 demonstrates that calibration source position errors may degrade the accuracy of estimation of satellite position. However, it also reveals that using the calibration emitters provides considerable improvement in the accuracy of position estimation by the satellites, although their positions are not obtained exactly.

**Proposition 10**  $\mathbf{CRB}^{(d)}(\mathbf{v}^0) \leq \mathbf{P}_2$ .

Proposition 10 is shown in Appendix I. Proposition 10 demonstrates that through applying the calibration TDOA measurements, the accuracy of calibration emitter localization can be improved.

## 5 Performance analysis ignoring position errors of satellites and calibration sources

In this section, two kinds of location MSE expressions under the altitude constraint are deduced analytically. The first location MSE provides the theoretical prediction when an estimator assumes that the satellite locations are precise, but in fact they have errors. The second location MSE provides the localization accuracy if an estimator assumes that the known calibration source locations are accurate, while in fact erroneous. The two location MSEs are compared to the corresponding CRBs and some insights are gained into the effects of position errors of satellites and calibration sources on the estimation performance.

Note that although similar location MSEs have been deduced (Lu and Ho, 2006b; Ho *et al.*, 2007; Ho and Yang, 2008; Yang and Ho, 2010b), these analyses did not involve an altitude constraint, and consequently cannot be directly applied here. In addition, these two location MSEs were not studied by Ho and Chan (1997).

### 5.1 Source location ignoring satellite position errors

The aim of this subsection is to quantify the performance degradation attributable to the ignorance of satellite position errors. The location MSE is analytically derived when satellite positions are assumed accurate but in fact they have errors. By comparing

$$\text{CRB}^{(d)} \begin{pmatrix} u^0 \\ s^0 \\ v^0 \end{pmatrix} = \begin{bmatrix} X^{(d)} & Y^{(d)} & \mathbf{O} \\ Y^{(d)T} & Z^{(d)} & W^{(d)T} \\ \mathbf{O} & W^{(d)} & T^{(d)} \end{bmatrix}^{-1} - \frac{\begin{bmatrix} X^{(d)} & Y^{(d)} & \mathbf{O} \\ Y^{(d)T} & Z^{(d)} & W^{(d)T} \\ \mathbf{O} & W^{(d)} & T^{(d)} \end{bmatrix}^{-1} \omega^{(d)} \omega^{(d)T} \begin{bmatrix} X^{(d)} & Y^{(d)} & \mathbf{O} \\ Y^{(d)T} & Z^{(d)} & W^{(d)T} \\ \mathbf{O} & W^{(d)} & T^{(d)} \end{bmatrix}^{-1}}{\omega^{(d)T} \begin{bmatrix} X^{(d)} & Y^{(d)} & \mathbf{O} \\ Y^{(d)T} & Z^{(d)} & W^{(d)T} \\ \mathbf{O} & W^{(d)} & T^{(d)} \end{bmatrix}^{-1} \omega^{(d)}} \quad (54)$$

$$\text{CRB}^{(d)} \begin{pmatrix} u^0 \\ s^0 \\ v^0 \end{pmatrix} = \begin{bmatrix} \Phi(Du^0) & \mathbf{O}_{3 \times 3M} & \mathbf{O}_{3 \times 3N} \\ \mathbf{O}_{3M \times 2} & I_{3M} & \mathbf{O}_{3M \times 3N} \\ \mathbf{O}_{3N \times 2} & \mathbf{O}_{3N \times 3M} & I_{3N} \end{bmatrix} \cdot \left[ \begin{bmatrix} \Phi^T(Du^0) & \mathbf{O}_{2 \times 3M} & \mathbf{O}_{2 \times 3N} \\ \mathbf{O}_{3M \times 3} & I_{3M} & \mathbf{O}_{3M \times 3N} \\ \mathbf{O}_{3N \times 3} & \mathbf{O}_{3N \times 3M} & I_{3N} \end{bmatrix} \begin{bmatrix} X^{(d)} & Y^{(d)} & \mathbf{O} \\ Y^{(d)T} & Z^{(d)} & W^{(d)T} \\ \mathbf{O} & W^{(d)} & T^{(d)} \end{bmatrix} \begin{bmatrix} \Phi(Du^0) & \mathbf{O}_{3 \times 3M} & \mathbf{O}_{3 \times 3N} \\ \mathbf{O}_{3M \times 2} & I_{3M} & \mathbf{O}_{3M \times 3N} \\ \mathbf{O}_{3N \times 2} & \mathbf{O}_{3N \times 3M} & I_{3N} \end{bmatrix} \right]^{-1} \begin{bmatrix} \Phi^T(Du^0) & \mathbf{O}_{2 \times 3M} & \mathbf{O}_{2 \times 3N} \\ \mathbf{O}_{3M \times 3} & I_{3M} & \mathbf{O}_{3M \times 3N} \\ \mathbf{O}_{3N \times 3} & \mathbf{O}_{3N \times 3M} & I_{3N} \end{bmatrix} \quad (56)$$

$$\begin{aligned} \text{CRB}^{(d)}(u^0) &= \Phi(Du^0) \{ \Phi^T(Du^0) [X^{(d)} - Y^{(d)}(Z^{(d)} - W^{(d)T}(T^{(d)})^{-1}W^{(d)})^{-1}Y^{(d)T}] \Phi(Du^0) \}^{-1} \Phi^T(Du^0) \\ &= \Phi(Du^0) (\Phi^T(Du^0) X^{(d)} \Phi(Du^0))^{-1} \Phi^T(Du^0) + \Phi(Du^0) (\Phi^T(Du^0) X^{(d)} \Phi(Du^0))^{-1} \Phi^T(Du^0) \\ &\quad \cdot Y^{(d)} [Z^{(d)} - Y^{(d)T} \Phi(Du^0) (\Phi^T(Du^0) X^{(d)} \Phi(Du^0))^{-1} \Phi^T(Du^0) Y^{(d)} - W^{(d)T} (T^{(d)})^{-1} W^{(d)}]^{-1} \\ &\quad \cdot Y^{(d)T} \Phi(Du^0) (\Phi^T(Du^0) X^{(d)} \Phi(Du^0))^{-1} \Phi^T(Du^0). \end{aligned} \quad (57)$$

$$\begin{aligned} \text{CRB}^{(d)}(s^0) &= [Z^{(d)} - W^{(d)T}(T^{(d)})^{-1}W^{(d)} - Y^{(d)T} \Phi(Du^0) (\Phi^T(Du^0) X^{(d)} \Phi(Du^0))^{-1} \Phi^T(Du^0) Y^{(d)}]^{-1} \\ &= (Z^{(d)} - W^{(d)T}(T^{(d)})^{-1}W^{(d)})^{-1} + (Z^{(d)} - W^{(d)T}(T^{(d)})^{-1}W^{(d)})^{-1} Y^{(d)T} \Phi(Du^0) \\ &\quad \cdot \{ \Phi^T(Du^0) [X^{(d)} - Y^{(d)}(Z^{(d)} - W^{(d)T}(T^{(d)})^{-1}W^{(d)})^{-1}Y^{(d)T}] \Phi(Du^0) \}^{-1} \\ &\quad \cdot \Phi^T(Du^0) Y^{(d)} (Z^{(d)} - W^{(d)T}(T^{(d)})^{-1}W^{(d)})^{-1}. \end{aligned} \quad (58)$$

$$\begin{aligned} \text{CRB}^{(d)}(v^0) &= [T^{(d)} - W^{(d)}(Z^{(d)} - Y^{(d)T} \Phi(Du^0) (\Phi^T(Du^0) X^{(d)} \Phi(Du^0))^{-1} \Phi^T(Du^0) Y^{(d)})^{-1} W^{(d)T}]^{-1} \\ &= (T^{(d)})^{-1} + (T^{(d)})^{-1} W^{(d)} (Z^{(d)} - Y^{(d)T} \Phi(Du^0) (\Phi^T(Du^0) X^{(d)} \Phi(Du^0))^{-1} \Phi^T(Du^0) Y^{(d)}) \\ &\quad - W^{(d)T} (T^{(d)})^{-1} W^{(d)} W^{(d)T} (T^{(d)})^{-1}. \end{aligned} \quad (59)$$

the location MSE with the CRB in the absence of satellite position errors, we can assess how much degradation of emitter location accuracy is expected with respect to the amount of satellite position errors. In addition, comparing the location MSE with the CRB in the presence of satellite position errors allows us to decide whether a new algorithm to account for satellite location errors is necessary to improve the accuracy of emitter location. For convenience, the investigation provided here is a first-order perturbation analysis.

Hence, the result obtained in this subsection is valid, only if the levels of both the TDOA

measurement noise and the satellite position perturbations are not too large.

Assume the estimate of  $u^0$  is denoted as  $\hat{u}_{\text{opt}}^{(1)}$  if the satellite position errors exist but are neglected by the estimator. Consequently,  $\hat{u}_{\text{opt}}^{(1)}$  is the solution to the following constrained minimization problem:

$$\begin{aligned} \min_{x \in \mathbb{R}^{3M}} \{ (\Delta t^u - h(x, s))^T Q_1^{-1} (\Delta t^u - h(x, s)) \} \quad (63) \\ \text{s.t. } x^T D x = r_e^2. \end{aligned}$$

To proceed, we define  $\tilde{u}_{\text{opt}}^{(1)}$  as the estimation error of  $\hat{u}_{\text{opt}}^{(1)}$ , i.e.,  $\tilde{u}_{\text{opt}}^{(1)} = \hat{u}_{\text{opt}}^{(1)} - u^0$ . Then, with the first-order

approximation,  $\tilde{\mathbf{u}}_{\text{opt}}^{(1)}$  is the solution to the following problem:

$$\begin{aligned} \min_{\mathbf{x} \in \mathbb{R}^{3M}} \{ & (\Delta \tilde{\mathbf{t}}^u - \mathbf{H}_1(\mathbf{u}^0, \mathbf{s}^0) \mathbf{x} - \mathbf{H}_2(\mathbf{u}^0, \mathbf{s}^0) \tilde{\mathbf{s}})^T \\ & \mathbf{Q}_1^{-1} (\Delta \tilde{\mathbf{t}}^u - \mathbf{H}_1(\mathbf{u}^0, \mathbf{s}^0) \mathbf{x} - \mathbf{H}_2(\mathbf{u}^0, \mathbf{s}^0) \tilde{\mathbf{s}}) \} \\ \text{s.t. } & \mathbf{x}^T \mathbf{D} \mathbf{u}^0 = \mathbf{x}^T \boldsymbol{\omega}^{(a)} = 0, \end{aligned} \quad (64)$$

which can be solved via the method of Lagrangian multipliers.

First, the auxiliary cost function of the constrained problem is formulated as

$$\begin{aligned} J^{(1)}(\mathbf{x}, \lambda) = & (\Delta \tilde{\mathbf{t}}^u - \mathbf{H}_1(\mathbf{u}^0, \mathbf{s}^0) \mathbf{x} - \mathbf{H}_2(\mathbf{u}^0, \mathbf{s}^0) \tilde{\mathbf{s}})^T \\ & \cdot \mathbf{Q}_1^{-1} (\Delta \tilde{\mathbf{t}}^u - \mathbf{H}_1(\mathbf{u}^0, \mathbf{s}^0) \mathbf{x} - \mathbf{H}_2(\mathbf{u}^0, \mathbf{s}^0) \tilde{\mathbf{s}}) \\ & + \lambda \mathbf{x}^T \boldsymbol{\omega}^{(a)}, \end{aligned} \quad (65)$$

where  $\tilde{\lambda}$  is the Lagrangian multiplier. Setting derivatives of  $J^{(1)}(\tilde{\mathbf{u}}, \tilde{\lambda})$  with respect to  $\tilde{\mathbf{u}}$  and  $\tilde{\lambda}$  to zero yields

$$\left\{ \begin{aligned} \frac{\partial J^{(1)}(\mathbf{x}, \lambda)}{\partial \mathbf{x}} \Big|_{\substack{\mathbf{x}=\tilde{\mathbf{u}}_{\text{opt}}^{(1)} \\ \lambda=\tilde{\lambda}_{\text{opt}}^{(1)}}} &= -2\mathbf{H}_1^T(\mathbf{u}^0, \mathbf{s}^0) \mathbf{Q}_1^{-1} \\ & \cdot (\Delta \tilde{\mathbf{t}}^u - \mathbf{H}_1(\mathbf{u}^0, \mathbf{s}^0) \tilde{\mathbf{u}}_{\text{opt}}^{(1)} \\ & - \mathbf{H}_2(\mathbf{u}^0, \mathbf{s}^0) \tilde{\mathbf{s}}) + \tilde{\lambda}_{\text{opt}}^{(1)} \boldsymbol{\omega}^{(a)} \\ & = \mathbf{O}_{3 \times 1}, \\ \frac{\partial J^{(1)}(\mathbf{x}, \lambda)}{\partial \lambda} \Big|_{\substack{\mathbf{x}=\tilde{\mathbf{u}}_{\text{opt}}^{(1)} \\ \lambda=\tilde{\lambda}_{\text{opt}}^{(1)}}} &= \tilde{\mathbf{u}}_{\text{opt}}^{(1)T} \boldsymbol{\omega}^{(a)} = 0. \end{aligned} \right. \quad (66)$$

From the first equality in Eq. (66), we conclude that

$$\begin{aligned} \tilde{\mathbf{u}}_{\text{opt}}^{(1)} = & (\mathbf{H}_1^T(\mathbf{u}^0, \mathbf{s}^0) \mathbf{Q}_1^{-1} \mathbf{H}_1(\mathbf{u}^0, \mathbf{s}^0))^{-1} \mathbf{H}_1^T(\mathbf{u}^0, \mathbf{s}^0) \\ & \cdot \mathbf{Q}_1^{-1} (\Delta \tilde{\mathbf{t}}^u - \mathbf{H}_2(\mathbf{u}^0, \mathbf{s}^0) \tilde{\mathbf{s}}) \\ & - \tilde{\lambda}_{\text{opt}}^{(1)} (\mathbf{H}_1^T(\mathbf{u}^0, \mathbf{s}^0) \mathbf{Q}_1^{-1} \mathbf{H}_1(\mathbf{u}^0, \mathbf{s}^0))^{-1} \boldsymbol{\omega}^{(a)} / 2 \\ = & (\mathbf{X}^{(b)})^{-1} (\mathbf{H}_1^T(\mathbf{u}^0, \mathbf{s}^0) \mathbf{Q}_1^{-1} \Delta \tilde{\mathbf{t}}^u - \mathbf{Y}^{(b)} \tilde{\mathbf{s}}) \\ & - \tilde{\lambda}_{\text{opt}}^{(1)} (\mathbf{X}^{(b)})^{-1} \boldsymbol{\omega}^{(a)} / 2. \end{aligned} \quad (67)$$

Premultiplying Eq. (67) with  $\boldsymbol{\omega}^{(a)T}$  and using the constraint equality  $\tilde{\mathbf{u}}_{\text{opt}}^{(1)T} \boldsymbol{\omega}^{(a)} = 0$ , we arrive at

$$\tilde{\lambda}_{\text{opt}}^{(1)} = \frac{2\boldsymbol{\omega}^{(a)T} (\mathbf{X}^{(b)})^{-1} (\mathbf{H}_1^T(\mathbf{u}^0, \mathbf{s}^0) \mathbf{Q}_1^{-1} \Delta \tilde{\mathbf{t}}^u - \mathbf{Y}^{(b)} \tilde{\mathbf{s}})}{\boldsymbol{\omega}^{(a)T} (\mathbf{X}^{(b)})^{-1} \boldsymbol{\omega}^{(a)}}. \quad (68)$$

Putting Eq. (68) back into Eq. (67) leads to

$$\begin{aligned} \tilde{\mathbf{u}}_{\text{opt}}^{(1)} = & \left( \mathbf{I}_3 - \frac{(\mathbf{X}^{(b)})^{-1} \boldsymbol{\omega}^{(a)} \boldsymbol{\omega}^{(a)T}}{\boldsymbol{\omega}^{(a)T} (\mathbf{X}^{(b)})^{-1} \boldsymbol{\omega}^{(a)}} \right) (\mathbf{X}^{(b)})^{-1} \\ & \cdot (\mathbf{H}_1^T(\mathbf{u}^0, \mathbf{s}^0) \mathbf{Q}_1^{-1} \Delta \tilde{\mathbf{t}}^u - \mathbf{Y}^{(b)} \tilde{\mathbf{s}}). \end{aligned} \quad (69)$$

Then, the location MSE matrix of  $\hat{\mathbf{u}}_{\text{opt}}^{(1)}$  can be obtained by

$$\begin{aligned} \mathbf{MSE}(\hat{\mathbf{u}}_{\text{opt}}^{(1)}) = & E[\tilde{\mathbf{u}}_{\text{opt}}^{(1)} \tilde{\mathbf{u}}_{\text{opt}}^{(1)T}] \\ = & \left( \mathbf{I}_3 - \frac{(\mathbf{X}^{(b)})^{-1} \boldsymbol{\omega}^{(a)} \boldsymbol{\omega}^{(a)T}}{\boldsymbol{\omega}^{(a)T} (\mathbf{X}^{(b)})^{-1} \boldsymbol{\omega}^{(a)}} \right) (\mathbf{X}^{(b)})^{-1} \\ & + \left( \mathbf{I}_3 - \frac{(\mathbf{X}^{(b)})^{-1} \boldsymbol{\omega}^{(a)} \boldsymbol{\omega}^{(a)T}}{\boldsymbol{\omega}^{(a)T} (\mathbf{X}^{(b)})^{-1} \boldsymbol{\omega}^{(a)}} \right) (\mathbf{X}^{(b)})^{-1} \mathbf{Y}^{(b)} \mathbf{Q}_2 \\ & \cdot \mathbf{Y}^{(b)T} (\mathbf{X}^{(b)})^{-1} \left( \mathbf{I}_3 - \frac{\boldsymbol{\omega}^{(a)} \boldsymbol{\omega}^{(a)T} (\mathbf{X}^{(b)})^{-1}}{\boldsymbol{\omega}^{(a)T} (\mathbf{X}^{(b)})^{-1} \boldsymbol{\omega}^{(a)}} \right) \\ = & \mathbf{CRB}^{(a)}(\mathbf{u}^0) + \mathbf{CRB}^{(a)}(\mathbf{u}^0) \mathbf{Y}^{(b)} \mathbf{Q}_2 \mathbf{Y}^{(b)T} \\ & \cdot \mathbf{CRB}^{(a)}(\mathbf{u}^0). \end{aligned} \quad (70)$$

From Eq. (70), it follows that  $\mathbf{MSE}(\hat{\mathbf{u}}_{\text{opt}}^{(1)}) \geq \mathbf{CRB}^{(a)}(\mathbf{u}^0)$ .

After further analysis, the following result can be drawn:

**Proposition 11**  $\mathbf{MSE}(\hat{\mathbf{u}}_{\text{opt}}^{(1)}) \geq \mathbf{CRB}^{(b)}(\mathbf{u}^0)$ .

Proposition 11 is proved in Appendix J. Proposition 11 indicates that an estimation algorithm to account for the satellite location errors is necessary to improve the accuracy of target location.

## 5.2 Source location mean-square errors without accounting for calibration source position errors

This subsection is devoted to determining the performance loss in location MSE when an estimator assumes that the known calibration source positions are precise, while in fact they are erroneous. By comparing location MSE with CRB when the calibration source positions are accurate, we can assess how much degradation of emitter location accuracy is expected with respect to the amount of calibration source position errors. Also, comparing location MSE with CRB in the presence of calibration source position errors allows us to decide whether a new algorithm to account for the calibration source location errors is necessary to improve the accuracy of target

location. Similar to the previous derivation, the theoretical formula provided here is a first-order perturbation method.

Assume the estimates of  $\mathbf{u}^0$  and  $\mathbf{s}^0$  are denoted as  $\hat{\mathbf{u}}_{\text{opt}}^{(2)}$  and  $\hat{\mathbf{s}}_{\text{opt}}^{(2)}$ , respectively, if calibration source position errors are present but are not considered by the estimator. As a consequence,  $\hat{\mathbf{u}}_{\text{opt}}^{(2)}$  and  $\hat{\mathbf{s}}_{\text{opt}}^{(2)}$  are the solution to the following constrained optimization problem:

$$\begin{aligned} \min_{\substack{\mathbf{x} \in \mathbb{R}^{3 \times 1} \\ \mathbf{y} \in \mathbb{R}^{3M \times 1}}} & \{(\Delta \mathbf{t}^u - \mathbf{h}(\mathbf{x}, \mathbf{y}))^T \mathbf{Q}_1^{-1} (\Delta \mathbf{t}^u - \mathbf{h}(\mathbf{x}, \mathbf{y})) \\ & + (\Delta \mathbf{t}^v - \mathbf{g}(\mathbf{v}, \mathbf{y}))^T \mathbf{P}_1^{-1} (\Delta \mathbf{t}^v - \mathbf{g}(\mathbf{v}, \mathbf{y})) \\ & + (\mathbf{s} - \mathbf{y})^T \mathbf{Q}_2^{-1} (\mathbf{s} - \mathbf{y})\} \\ \text{s.t. } & \mathbf{x}^T \mathbf{D} \mathbf{x} = r_e^2. \end{aligned} \quad (71)$$

To proceed, we define  $\tilde{\mathbf{u}}_{\text{opt}}^{(2)}$  and  $\tilde{\mathbf{s}}_{\text{opt}}^{(2)}$  as the estimation error of  $\hat{\mathbf{u}}_{\text{opt}}^{(2)}$  and  $\hat{\mathbf{s}}_{\text{opt}}^{(2)}$ , respectively, i.e.,  $\tilde{\mathbf{u}}_{\text{opt}}^{(2)} = \hat{\mathbf{u}}_{\text{opt}}^{(2)} - \mathbf{u}^0$ , and  $\tilde{\mathbf{s}}_{\text{opt}}^{(2)} = \hat{\mathbf{s}}_{\text{opt}}^{(2)} - \mathbf{s}^0$ . Then, with the first-order approximation,  $\tilde{\mathbf{u}}_{\text{opt}}^{(2)}$  and  $\tilde{\mathbf{s}}_{\text{opt}}^{(2)}$  are the solution to the following problem:

$$\begin{aligned} \min_{\substack{\mathbf{x} \in \mathbb{R}^{3 \times 1} \\ \mathbf{y} \in \mathbb{R}^{3M \times 1}}} & \{(\Delta \tilde{\mathbf{t}}^u - \mathbf{H}_1(\mathbf{u}^0, \mathbf{s}^0) \mathbf{x} - \mathbf{H}_2(\mathbf{u}^0, \mathbf{s}^0) \mathbf{y})^T \mathbf{Q}_1^{-1} \\ & \cdot (\Delta \tilde{\mathbf{t}}^u - \mathbf{H}_1(\mathbf{u}^0, \mathbf{s}^0) \mathbf{x} - \mathbf{H}_2(\mathbf{u}^0, \mathbf{s}^0) \mathbf{y}) \\ & + (\Delta \tilde{\mathbf{t}}^v - \mathbf{G}_1(\mathbf{v}^0, \mathbf{s}^0) \tilde{\mathbf{v}} - \mathbf{G}_2(\mathbf{v}^0, \mathbf{s}^0) \mathbf{y})^T \mathbf{P}_1^{-1} \\ & \cdot (\Delta \tilde{\mathbf{t}}^v - \mathbf{G}_1(\mathbf{v}^0, \mathbf{s}^0) \tilde{\mathbf{v}} - \mathbf{G}_2(\mathbf{v}^0, \mathbf{s}^0) \mathbf{y}) \\ & + (\tilde{\mathbf{s}} - \mathbf{y})^T \mathbf{Q}_2^{-1} (\tilde{\mathbf{s}} - \mathbf{y})\} \\ \text{s.t. } & \mathbf{x}^T \mathbf{D} \mathbf{u}^0 = \mathbf{x}^T \boldsymbol{\omega}^{(a)} = 0, \end{aligned} \quad (72)$$

which can also be solved via the method of Lagrange multipliers.

First, the auxiliary cost function of the constrained problem is formulated as Eq. (73).

Taking the gradient of  $J^{(2)}(\mathbf{x}, \mathbf{y}, \lambda)$  with respect to  $\mathbf{x}$ ,  $\mathbf{y}$ , and  $\lambda$  and equating the results to zero yield Eq. (74), where the first and second equalities produce Eqs. (75) and (76).

Inserting Eq. (76) into Eq. (75) yields Eq. (77).

Premultiplying Eq. (77) with  $\boldsymbol{\omega}^{(a)T}$  and using the constraint equality  $\tilde{\mathbf{u}}_{\text{opt}}^{(2)T} \boldsymbol{\omega}^{(a)} = 0$  lead to Eq. (78).

Putting Eq. (78) back into Eq. (77) yields Eq. (79).

Consequently, the location MSE matrix of  $\hat{\mathbf{u}}_{\text{opt}}^{(2)}$  can be written by Eq. (80).

From Eq. (80), it follows that  $\mathbf{MSE}(\hat{\mathbf{u}}_{\text{opt}}^{(2)}) \geq \mathbf{CRB}^{(c)}(\mathbf{u}^0)$ . After further analysis, Proposition 12 can be obtained.

Eqs. (73)–(80) are shown on pages 1374–1375.

**Proposition 12**  $\mathbf{MSE}(\hat{\mathbf{u}}_{\text{opt}}^{(2)}) \geq \mathbf{CRB}^{(d)}(\mathbf{u}^0)$ .

Proposition 12 is proved in Appendix K. Proposition 12 indicates that an estimator should account for the calibration source position errors to decrease the estimation variance of the target location.

## 6 Simulation

In this section, a variety of simulations are reported to demonstrate the effectiveness of the analytical analysis in this paper. The maximum likelihood (ML) criterion was chosen as an estimator, which can be solved numerically through the Taylor-series iteration with the altitude constraint. Moreover, the initial solution was close to the true value to avoid the divergence problem, because the primary aim here was to validate the theoretical analysis presented previously. On the other hand, since TDOA is equivalent to the range difference of arrival (RDOA) after multiplying by the known signal propagation speed, RDOA was used instead of TDOA hereafter for simplicity.

In our simulation study, the emitter longitude and latitude were chosen as 123.78 °E and 30.22 °N, respectively. The emitter altitude was set to zero. The location of the observer on the Earth had a longitude of 120.47 °E and a latitude of 31.14 °N. Assuming that a total of five satellites were used for geolocation, their longitudes were set to 118.46 °E, 123.42 °E, 111.74 °E, 128.32 °E, and 132.31 °E, respectively, and their latitudes to 25.49 °N, 21.87 °N, 20.32 °N, 23.65 °N, and 26.46 °N, respectively. The following simulations were conducted for four geolocation scenarios, as described in Section 4. The CRBs corresponding to the four cases are denoted as CRB-a, CRB-b, CRB-c, and CRB-d, respectively.

### 6.1 Scenario 1: in absence of satellite position errors

In this scenario, the satellite positions are accurately known and only RDOA measurement errors are



$$\begin{aligned}
\tilde{\mathbf{u}}_{\text{opt}}^{(2)} = & \left( \mathbf{I}_3 - \frac{(\mathbf{X}^{(d)} - \mathbf{Y}^{(d)}(\mathbf{Z}^{(d)})^{-1}\mathbf{Y}^{(d)\text{T}})^{-1}\boldsymbol{\omega}^{(a)}\boldsymbol{\omega}^{(a)\text{T}}}{\boldsymbol{\omega}^{(a)\text{T}}(\mathbf{X}^{(d)} - \mathbf{Y}^{(d)}(\mathbf{Z}^{(d)})^{-1}\mathbf{Y}^{(d)\text{T}})^{-1}\boldsymbol{\omega}^{(a)}} \right) (\mathbf{X}^{(d)} - \mathbf{Y}^{(d)}(\mathbf{Z}^{(d)})^{-1}\mathbf{Y}^{(d)\text{T}})^{-1} (\mathbf{H}_1^{\text{T}}(\mathbf{u}^0, \mathbf{s}^0) \\
& - \mathbf{Y}^{(d)}(\mathbf{Z}^{(d)})^{-1}\mathbf{H}_2^{\text{T}}(\mathbf{u}^0, \mathbf{s}^0)) \mathbf{Q}_1^{-1} \Delta \tilde{\mathbf{t}}^u \\
& - \left( \mathbf{I}_3 - \frac{(\mathbf{X}^{(d)} - \mathbf{Y}^{(d)}(\mathbf{Z}^{(d)})^{-1}\mathbf{Y}^{(d)\text{T}})^{-1}\boldsymbol{\omega}^{(a)}\boldsymbol{\omega}^{(a)\text{T}}}{\boldsymbol{\omega}^{(a)\text{T}}(\mathbf{X}^{(d)} - \mathbf{Y}^{(d)}(\mathbf{Z}^{(d)})^{-1}\mathbf{Y}^{(d)\text{T}})^{-1}\boldsymbol{\omega}^{(a)}} \right) (\mathbf{X}^{(d)} - \mathbf{Y}^{(d)}(\mathbf{Z}^{(d)})^{-1}\mathbf{Y}^{(d)\text{T}})^{-1} \mathbf{Y}^{(d)}(\mathbf{Z}^{(d)})^{-1} \mathbf{G}_2^{\text{T}}(\mathbf{v}^0, \mathbf{s}^0) \mathbf{P}_1^{-1} \Delta \tilde{\mathbf{t}}^v \quad (79) \\
& - \left( \mathbf{I}_3 - \frac{(\mathbf{X}^{(d)} - \mathbf{Y}^{(d)}(\mathbf{Z}^{(d)})^{-1}\mathbf{Y}^{(d)\text{T}})^{-1}\boldsymbol{\omega}^{(a)}\boldsymbol{\omega}^{(a)\text{T}}}{\boldsymbol{\omega}^{(a)\text{T}}(\mathbf{X}^{(d)} - \mathbf{Y}^{(d)}(\mathbf{Z}^{(d)})^{-1}\mathbf{Y}^{(d)\text{T}})^{-1}\boldsymbol{\omega}^{(a)}} \right) (\mathbf{X}^{(d)} - \mathbf{Y}^{(d)}(\mathbf{Z}^{(d)})^{-1}\mathbf{Y}^{(d)\text{T}})^{-1} \mathbf{Y}^{(d)}(\mathbf{Z}^{(d)})^{-1} \mathbf{Q}_2^{-1} \tilde{\mathbf{s}} \\
& + \left( \mathbf{I}_3 - \frac{(\mathbf{X}^{(d)} - \mathbf{Y}^{(d)}(\mathbf{Z}^{(d)})^{-1}\mathbf{Y}^{(d)\text{T}})^{-1}\boldsymbol{\omega}^{(a)}\boldsymbol{\omega}^{(a)\text{T}}}{\boldsymbol{\omega}^{(a)\text{T}}(\mathbf{X}^{(d)} - \mathbf{Y}^{(d)}(\mathbf{Z}^{(d)})^{-1}\mathbf{Y}^{(d)\text{T}})^{-1}\boldsymbol{\omega}^{(a)}} \right) (\mathbf{X}^{(d)} - \mathbf{Y}^{(d)}(\mathbf{Z}^{(d)})^{-1}\mathbf{Y}^{(d)\text{T}})^{-1} \mathbf{Y}^{(d)}(\mathbf{Z}^{(d)})^{-1} \mathbf{W}^{(d)\text{T}} \tilde{\mathbf{v}}.
\end{aligned}$$

$$\begin{aligned}
\text{MSE}(\hat{\mathbf{u}}_{\text{opt}}^{(2)}) = E[\tilde{\mathbf{u}}_{\text{opt}}^{(2)}\tilde{\mathbf{u}}_{\text{opt}}^{(2)\text{T}}] = & \left( \mathbf{I}_3 - \frac{(\mathbf{X}^{(d)} - \mathbf{Y}^{(d)}(\mathbf{Z}^{(d)})^{-1}\mathbf{Y}^{(d)\text{T}})^{-1}\boldsymbol{\omega}^{(a)}\boldsymbol{\omega}^{(a)\text{T}}}{\boldsymbol{\omega}^{(a)\text{T}}(\mathbf{X}^{(d)} - \mathbf{Y}^{(d)}(\mathbf{Z}^{(d)})^{-1}\mathbf{Y}^{(d)\text{T}})^{-1}\boldsymbol{\omega}^{(a)}} \right) (\mathbf{X}^{(d)} - \mathbf{Y}^{(d)}(\mathbf{Z}^{(d)})^{-1}\mathbf{Y}^{(d)\text{T}})^{-1} \\
& + \left( \mathbf{I}_3 - \frac{(\mathbf{X}^{(d)} - \mathbf{Y}^{(d)}(\mathbf{Z}^{(d)})^{-1}\mathbf{Y}^{(d)\text{T}})^{-1}\boldsymbol{\omega}^{(a)}\boldsymbol{\omega}^{(a)\text{T}}}{\boldsymbol{\omega}^{(a)\text{T}}(\mathbf{X}^{(d)} - \mathbf{Y}^{(d)}(\mathbf{Z}^{(d)})^{-1}\mathbf{Y}^{(d)\text{T}})^{-1}\boldsymbol{\omega}^{(a)}} \right) (\mathbf{X}^{(d)} - \mathbf{Y}^{(d)}(\mathbf{Z}^{(d)})^{-1}\mathbf{Y}^{(d)\text{T}})^{-1} \mathbf{Y}^{(d)}(\mathbf{Z}^{(d)})^{-1} \mathbf{W}^{(d)\text{T}} \mathbf{P}_2 \\
& \cdot \mathbf{W}^{(d)}(\mathbf{Z}^{(d)})^{-1} \mathbf{Y}^{(d)\text{T}} (\mathbf{X}^{(d)} - \mathbf{Y}^{(d)}(\mathbf{Z}^{(d)})^{-1}\mathbf{Y}^{(d)\text{T}})^{-1} \left( \mathbf{I}_3 - \frac{\boldsymbol{\omega}^{(a)}\boldsymbol{\omega}^{(a)\text{T}}(\mathbf{X}^{(d)} - \mathbf{Y}^{(d)}(\mathbf{Z}^{(d)})^{-1}\mathbf{Y}^{(d)\text{T}})^{-1}}{\boldsymbol{\omega}^{(a)\text{T}}(\mathbf{X}^{(d)} - \mathbf{Y}^{(d)}(\mathbf{Z}^{(d)})^{-1}\mathbf{Y}^{(d)\text{T}})^{-1}\boldsymbol{\omega}^{(a)}} \right) \\
& = \text{CRB}^{(c)}(\mathbf{u}^0) + \text{CRB}^{(c)}(\mathbf{u}^0) \mathbf{Y}^{(d)}(\mathbf{Z}^{(d)})^{-1} \mathbf{W}^{(d)\text{T}} \mathbf{P}_2 \mathbf{W}^{(d)}(\mathbf{Z}^{(d)})^{-1} \mathbf{Y}^{(d)\text{T}} \text{CRB}^{(c)}(\mathbf{u}^0).
\end{aligned} \quad (80)$$

present. Therefore, the calibration sources are not required for this case. The measured RDOAs were generated by adding to the true values with Gaussian noises with covariance matrix  $\mathbf{Q}_1 = \sigma_d^2 \bar{\mathbf{Q}}_1$ , where  $\sigma_d$  is the standard deviation of RDOA estimates. For simplicity,  $\bar{\mathbf{Q}}_1$  is equal to the matrix with diagonal elements equal to 1 and all other elements equal to 0.5 (Ho and Yang, 2008). The Taylor-series geolocation algorithm simulated here is called Taylor-a, which is devised to solve the following constrained ML estimator:

$$\begin{aligned}
\min_{\mathbf{x} \in \mathbb{R}^{3M}} [(\Delta \mathbf{t}^u - \mathbf{h}(\mathbf{x}, \mathbf{s}^0))^{\text{T}} \mathbf{Q}_1^{-1} (\Delta \mathbf{t}^u - \mathbf{h}(\mathbf{x}, \mathbf{s}^0))] \quad (81) \\
\text{s.t. } \mathbf{x}^{\text{T}} \mathbf{D} \mathbf{x} = r_e^2.
\end{aligned}$$

In the first example, the receivers were geosynchronous satellites which were 42 164 km from the Earth's center. In Fig. 1, the geolocation CRB and the root-mean-square-error (RMSE) for Taylor-a are displayed as functions of  $\sigma_d$ . In addition, to examine the gain in performance attributable to the altitude information, the unconstrained CRB and RMSE for the conventional Taylor-series iteration without altitude information are also plotted in Fig. 1. In the second example, the satellites were assumed to locate at a low Earth orbit (LEO) at a distance of 7179 km

from the Earth's center. The corresponding localization performance curves versus  $\sigma_d$  are plotted in Fig. 2.

## 6.2 Scenario 2: in the presence of satellite position errors and absence of calibration sources

In this scenario, both satellite position errors and RDOA measurement errors are present. The calibration sources are not employed, although they can decrease the localization errors in this case. The measured RDOAs were generated by adding to the true value Gaussian noises with covariance matrix  $\mathbf{Q}_1 = \sigma_d^2 \bar{\mathbf{Q}}_1$ , and  $\bar{\mathbf{Q}}_1$  was equal to the matrix with diagonal elements equal to 1 and all other elements equal to  $\alpha$ , which was changed from 0 to 0.9 in the following simulation. The noisy satellite positions were generated in a similar manner, and the covariance matrix was  $\mathbf{Q}_2 = \sigma_s^2 \mathbf{I}_{3M}$ , where  $\sigma_s$  is the standard deviation of prior measurements for satellite position. The Taylor-series geolocation algorithm simulated here is termed Taylor-b, which was developed to solve the following constrained ML estimator:

$$\begin{aligned}
\min_{\substack{\mathbf{x} \in \mathbb{R}^{3M} \\ \mathbf{y} \in \mathbb{R}^{3M \times 1}}} [(\Delta \mathbf{t}^u - \mathbf{h}(\mathbf{x}, \mathbf{y}))^{\text{T}} \mathbf{Q}_1^{-1} (\Delta \mathbf{t}^u - \mathbf{h}(\mathbf{x}, \mathbf{y})) \\
+ (\mathbf{s} - \mathbf{y})^{\text{T}} \mathbf{Q}_2^{-1} (\mathbf{s} - \mathbf{y})] \quad (82) \\
\text{s.t. } \mathbf{x}^{\text{T}} \mathbf{D} \mathbf{x} = r_e^2.
\end{aligned}$$



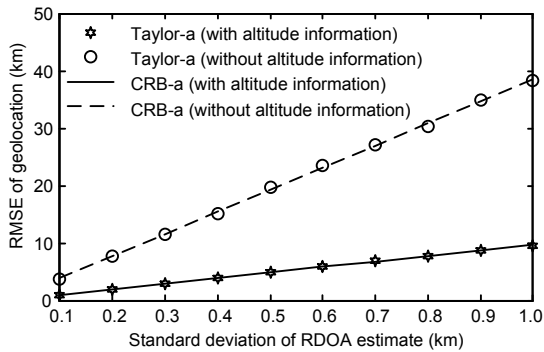


Fig. 1 RMSEs of geolocation versus standard deviations of RDOA estimates (geosynchronous satellite)

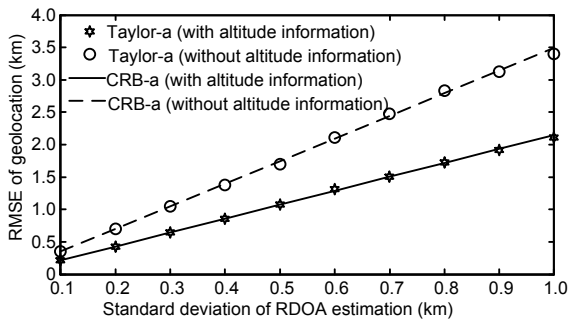


Fig. 2 RMSEs of geolocation versus standard deviations of RDOA estimates (LEO satellite)

Note that Taylor-a was also simulated in the presence of satellite position errors, because its empirical RMSE can be applied to support the effectiveness of Eq. (70).

The receivers were LEO satellites at a distance of 7179 km from the Earth’s center. In the first example,  $\sigma_s$  was fixed at 2 km and  $\alpha$  was set to zero. The performance curves for emitter localization and satellite position estimate versus  $\sigma_d$  are displayed in Figs. 3 and 4, respectively. In the second example,  $\sigma_d$  was fixed at 2 km and  $\alpha$  was set to zero. The same performance curves as a function of  $\sigma_s$  are plotted in Figs. 5 and 6. In the third example, both  $\sigma_s$  and  $\sigma_d$  were fixed at 2.5 km. Figs. 7 and 8 plot the corresponding performance curves as a function of  $\alpha$ .

Figs. 3–8 show that the empirical RMSE for Taylor-a in the presence of satellite location uncertainties matched the theoretical RMSE obtained by Eq. (70) well. Consequently, the effectiveness of Eq. (70) is verified. Moreover, the simulated RMSE values for Taylor-b were very close to those for CRB-b. As proved in Sections 4.2 and 5.1, the result of CRB-b is larger than that of CRB-a, but smaller

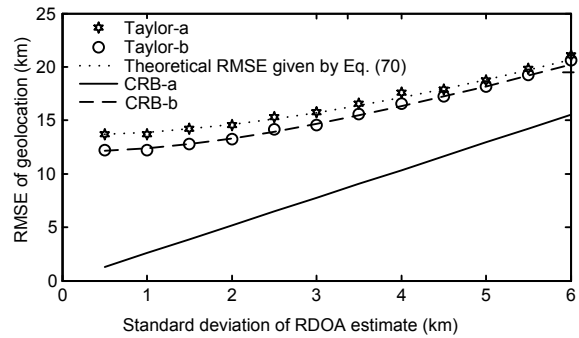


Fig. 3 RMSEs of geolocation versus standard deviations of RDOA estimates

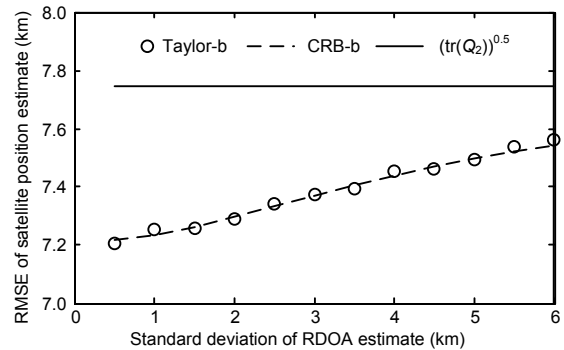


Fig. 4 RMSEs of satellite position estimates versus standard deviations of RDOA estimate

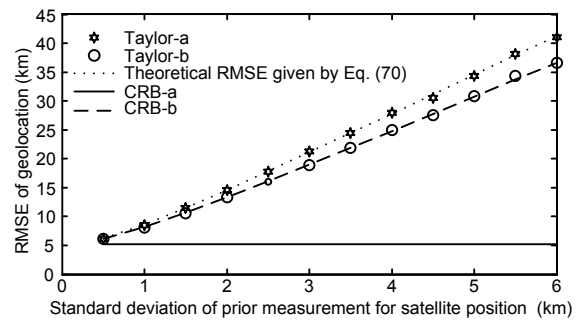
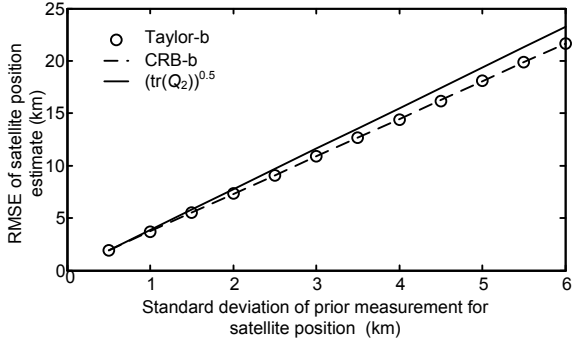
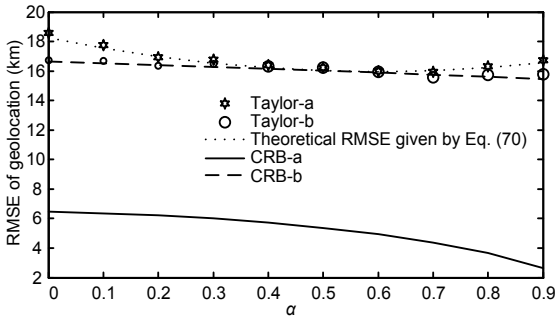


Fig. 5 RMSEs of geolocation versus standard deviations of prior measurements for satellite position

than the predicted RMSE determined by Eq. (70). The simulation results also demonstrated that the difference between CRB-a and CRB-b decreases as the standard deviation of RDOA estimates increases, and increases as the standard deviation of satellite position measurements increases. Finally, we conclude that compared to prior measurement, more accurate estimates of satellite position are available if RDOA measurements of the target source are effectively used.



**Fig. 6 RMSEs of satellite position estimates versus standard deviations of prior measurements for satellite position**



**Fig. 7 RMSEs of geolocation versus  $\alpha$**

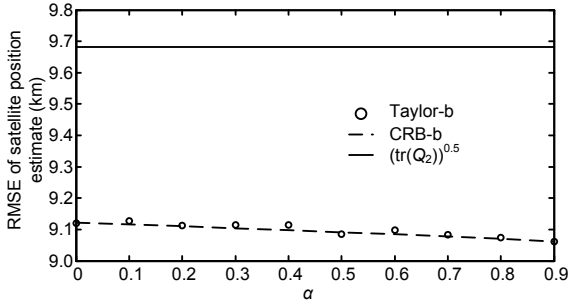


**Fig. 8 RMSEs of satellite position estimates versus  $\alpha$**

**6.3 Scenario 3: in the presence of calibration sources at accurate locations**

In this scenario, calibration sources with precise location information were employed to mitigate the effects of satellite position uncertainties. The RDOA measurement errors for calibration signals and target source have the same Gaussian distribution, and their covariance matrices are denoted as  $\mathbf{Q}_1 = \mathbf{P}_1 = \sigma_d^2 \bar{\mathbf{Q}}_1$ , where  $\bar{\mathbf{Q}}_1$  was set to the same value as in Section 6.1. The noisy satellite position measurements were

generated in the same manner as described in Section 6.2. The Taylor-series geolocation algorithm performed here is named Taylor-c, and was developed to solve the following constrained ML estimator:

$$\begin{aligned} \min_{\substack{\mathbf{x} \in \mathbb{R}^{3 \times 1} \\ \mathbf{y} \in \mathbb{R}^{3M \times 1}}} & [(\Delta \mathbf{t}^u - \mathbf{h}(\mathbf{x}, \mathbf{y}))^T \mathbf{Q}_1^{-1} (\Delta \mathbf{t}^u - \mathbf{h}(\mathbf{x}, \mathbf{y})) \\ & + (\Delta \mathbf{t}^v - \mathbf{g}(\mathbf{v}^0, \mathbf{y}))^T \mathbf{P}_1^{-1} (\Delta \mathbf{t}^v - \mathbf{g}(\mathbf{v}^0, \mathbf{y})) \\ & + (\mathbf{s} - \mathbf{y})^T \mathbf{Q}_2^{-1} (\mathbf{s} - \mathbf{y})] \quad (83) \\ \text{s.t. } & \mathbf{x}^T \mathbf{D} \mathbf{x} = r_c^2. \end{aligned}$$

A comparison of Taylor-b and Taylor-c is given in the following simulation.

The receivers were geosynchronous satellites at a distance of 42 164 km from the Earth’s center. In the first example,  $\sigma_s$  was fixed at 0.5 km. The performance curves for source localization and satellite position estimates versus  $\sigma_d$  are displayed in Figs. 9 and 10, respectively. In the second example,  $\sigma_d$  was fixed at 1.2 km. The same performance curves as a function of  $\sigma_s$  are shown in Figs. 11 and 12.

Figs. 9–12 show that the simulated RMSE values for Taylor-c match CRB-c very well. As proved in Section 4.3, the result of CRB-c is smaller than that of CRB-b, but larger than that of CRB-a. Moreover, the difference between the results of CRB-b and CRB-c decreases as the standard deviation of RDOA estimates increases, but increases as the standard deviation of satellite position measurements increases. In addition, the value of CRB-a remains the same when the standard deviation of satellite position measurements increases, because they are independent. Finally, the simulation results indicate that the use of calibration sources at accurate positions can lead to significantly improved estimation accuracy for satellite positions.

**6.4 Scenario 4: in the presence of calibration sources at inaccurate locations**

In this scenario, the calibration source positions are assumed to be perturbed by Gaussian noise, and the covariance matrix is denoted as  $\mathbf{P}_2 = \sigma_v^2 \mathbf{I}_{3N}$ , where  $\sigma_v$  is the standard deviation of prior measurements for calibration source position. The other three kinds of measurement errors were generated in the same way as in Section 6.3. The Taylor-series

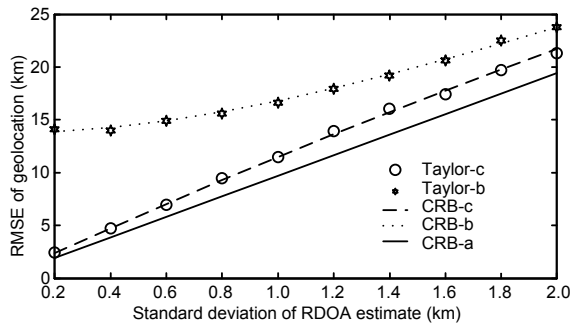


Fig. 9 RMSEs of geolocation versus standard deviations of RDOA estimates

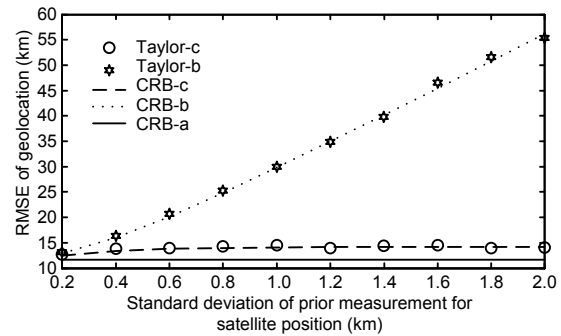


Fig. 11 RMSEs of geolocation versus standard deviations of prior measurements of satellite position

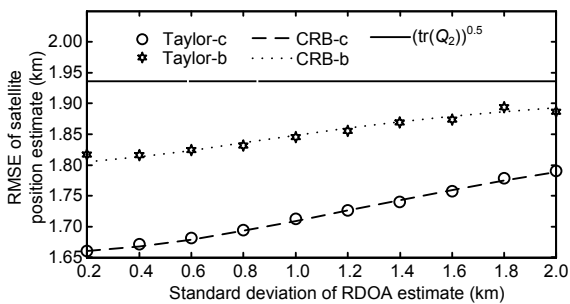


Fig. 10 RMSEs of satellite position estimates versus standard deviations of RDOA estimate

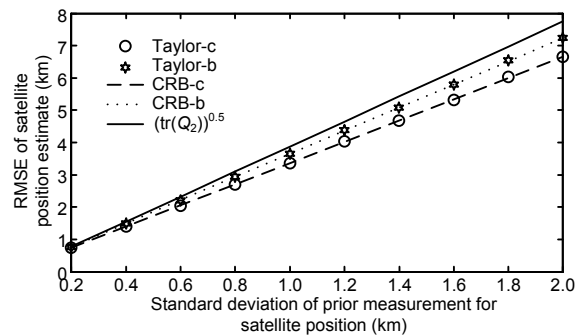


Fig. 12 RMSEs of satellite position estimates versus standard deviations of prior measurements for satellite position

geolocation algorithm performed here is termed Taylor-d, and was used to solve the following constrained ML estimator:

$$\begin{aligned} \min_{\substack{\mathbf{x} \in \mathbb{R}^{3 \times 1} \\ \mathbf{y} \in \mathbb{R}^{3M \times 1} \\ \mathbf{z} \in \mathbb{R}^{3N \times 1}}} & [(\Delta \mathbf{t}^u - \mathbf{h}(\mathbf{x}, \mathbf{y}))^T \mathbf{Q}_1^{-1} (\Delta \mathbf{t}^u - \mathbf{h}(\mathbf{x}, \mathbf{y})) \\ & + (\Delta \mathbf{t}^v - \mathbf{g}(\mathbf{z}, \mathbf{y}))^T \mathbf{P}_1^{-1} (\Delta \mathbf{t}^v - \mathbf{g}(\mathbf{z}, \mathbf{y})) \quad (84) \\ & + (\mathbf{s} - \mathbf{y})^T \mathbf{Q}_2^{-1} (\mathbf{s} - \mathbf{y})] \\ \text{s.t. } & \mathbf{x}^T \mathbf{D} \mathbf{x} = r_c^2. \end{aligned}$$

Note that Taylor-c was also simulated in the presence of calibration source position errors, because its empirical RMSE can be used to confirm the validity of Eq. (80).

The receivers were geosynchronous satellites at a distance of 42 164 km from the Earth’s center. In the first example,  $\sigma_s$  was fixed at 0.5 km and  $\sigma_v$  was set to 10 km. The performance curves for source localization, satellite position estimate, and calibration source position estimate versus  $\sigma_d$  are displayed in Figs. 13–15. In the second example,  $\sigma_d$  was fixed at 0.8 km and  $\sigma_v$  was set to 10 km. The same performance curves as a function of  $\sigma_s$  are plotted in

Figs. 16–18. In the third example,  $\sigma_d$  was fixed at 0.8 km and  $\sigma_s$  was set to 0.5 km. Figs. 19–21 show the corresponding performance curves as a function of  $\sigma_v$ .

Figs. 13–21 show agreement between the simulated RMSE values for Taylor-c in the presence of calibration source location errors and values predicted by Eq. (80). Hence, the validity of Eq. (80) is supported. Also, the empirical RMSE values for Taylor-d coincide with those for CRB-d. As proved in Sections 4.4 and 5.2, the result of CRB-d is larger than that of CRB-c, but smaller than that of CRB-b and the predicted RMSE determined by Eq. (80). Hence, it is possible to improve the localization accuracy by using the calibration sources at inaccurate locations. Moreover, the difference between the results of CRB-c and CRB-d decreases as the standard deviation of RDOA estimates increases, and increases as the standard deviation of satellite and calibration source position measurements increases. In addition, both results of CRB-b and CRB-c remain unchanged with the increase in the standard deviation of calibration source position measurements. The simulation

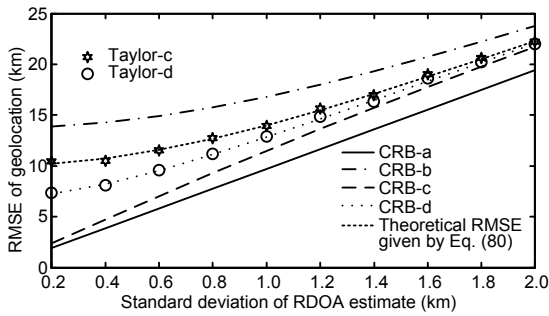


**Fig. 13 RMSEs of geolocation versus standard deviations of RDOA estimates**

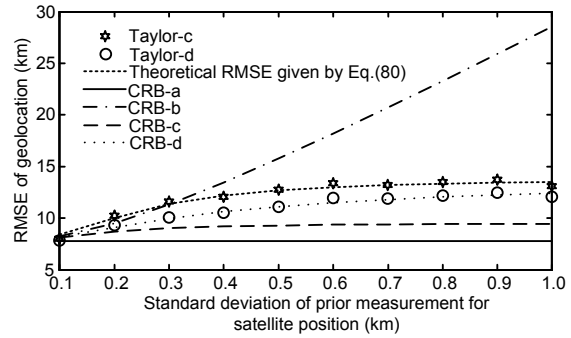


**Fig. 16 RMSEs of geolocation versus standard deviations of prior measurements of satellite position**

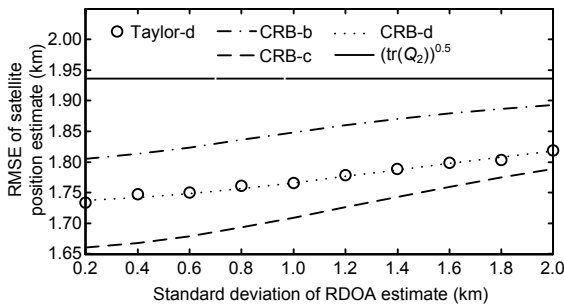


**Fig. 14 RMSEs of satellite position estimates versus standard deviations of RDOA estimates**

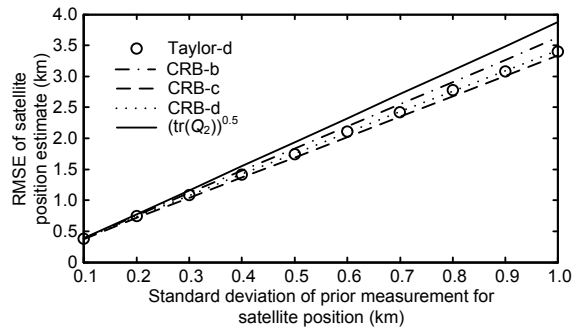


**Fig. 17 RMSEs of satellite position estimates versus standard deviations of prior measurements for satellite position**

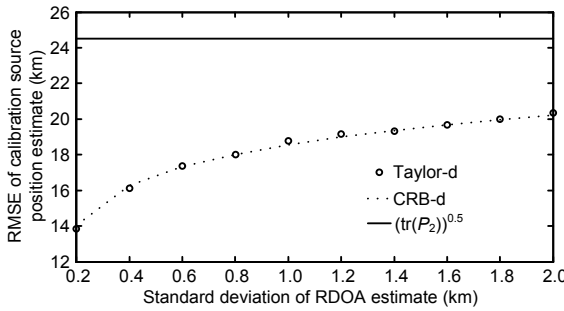


**Fig. 15 RMSEs of calibration source position estimates versus standard deviations of RDOA estimates**

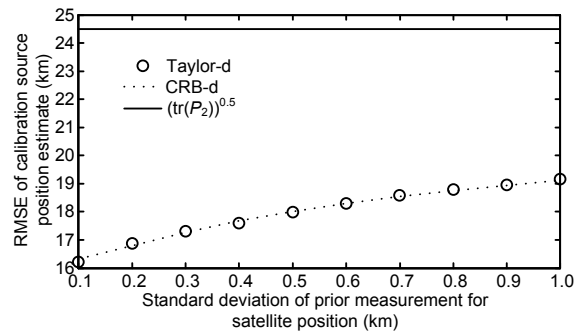


**Fig. 18 RMSEs of calibration source position estimates versus standard deviations of prior measurements of satellite position**

results demonstrate that the use of calibration sources at inaccurate positions can still lead to considerable improvement in the accuracy of satellite position estimates. Finally, we conclude that, as expected, more accurate calibration source position estimates are available if the RDOA measurements of the calibration source are effectively exploited.

## 7 Conclusions

In this paper, a systematic and comprehensive performance analysis of multi-satellite joint geolocation is presented. The theoretical analysis begins with

CRB derivations for four different geolocation scenarios with an altitude constraint and a Gaussian noise assumption. In scenario 1, only the TDOA measurement errors of the emitting source are considered, and satellite positions are assumed to have been accurately obtained. In scenario 2, TDOA measurement errors and satellite position perturbations are accounted for simultaneously. In scenario 3, it is assumed that some calibration sources with accurate position information are applied to reduce the

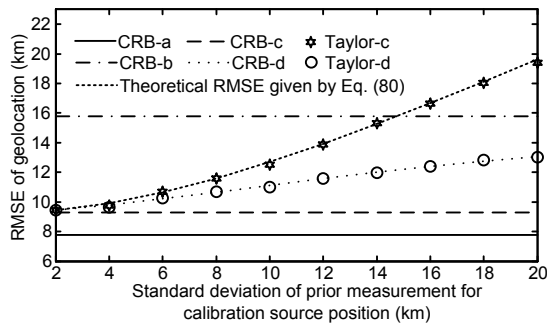


**Fig. 19** RMSEs of geolocation versus standard deviations of prior measurements of calibration source position

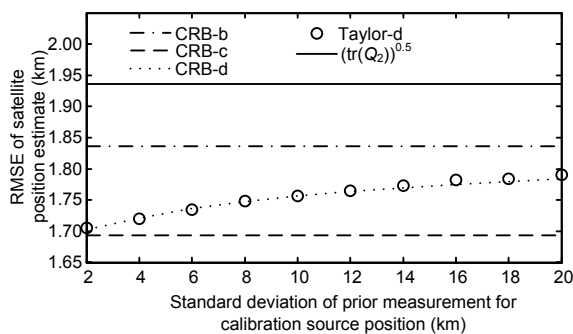


**Fig. 20** RMSEs of satellite position estimates versus standard deviations of prior measurements of calibration source position

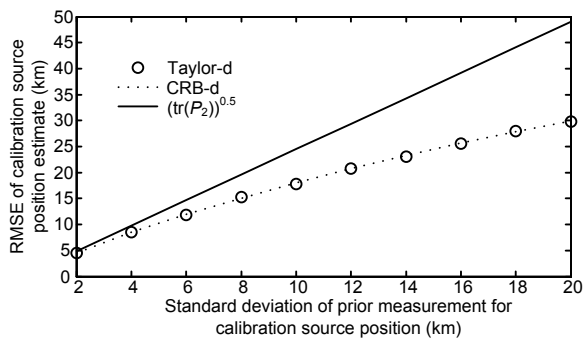


**Fig. 21** RMSEs of calibration source position estimates versus standard deviations of prior measurements for calibration source position

influences of satellite position perturbation. In scenario 4, several calibration sources at inaccurate locations are employed to alleviate satellite position uncertainties in target localization. By comparing the CRBs of the four localization scenarios stated above, some insights into the effects of various error sources on localization performance can be obtained. Also, two kinds of location MSE expressions under the altitude constraint are derived analytically through first-order error analysis and the Lagrangian multi-

pliers method. The first location MSE provides the theoretical prediction when an estimator assumes the satellite locations are precise but in fact they have errors. The second location MSE provides the localization accuracy if an estimator assumes that the known calibration source locations are accurate, while in fact they are erroneous. Then, the amount of reduction in the accuracy of localization due to the ignorance of satellite and calibration source location errors is quantified. Finally, a variety of simulations are reported, demonstrating the effectiveness of the theoretical analysis in this study.

## References

- Bardelli, R., Haworth, D., Smith, N., 1995. Interference localization for the EUTELSAT satellite system. *Proc. IEEE Int. Conf. on Globecom*, p.1641-1651. <http://dx.doi.org/10.1109/GLOCOM.1995.502690>
- Cheung, K.W., So, H.C., Ma, W.K., et al., 2006. A constrained least squares approach to mobile positioning: algorithms and optimality. *EURASIP J. Appl. Signal Process.*, **2006**: 1-23. <http://dx.doi.org/10.1155/ASP/2006/20858>
- Ding, W., 2014. The geolocation performance analysis for the constrained Taylor-series iteration in the presence of satellite orbit perturbations. *Sci. China Inform. Sci.*, **44**(2):231-253. <http://dx.doi.org/10.1360/112013-121>
- Ha, T.T., Robertson, R.C., 1987. Geostationary satellite navigation systems. *IEEE Trans. Aerosp. Electron. Syst.*, **23**(2):247-254. <http://dx.doi.org/10.1109/TAES.1987.313379>
- Haworth, D.P., Smith, N.G., Bardelli, R., et al., 1997. Interference localization for EUTELSAT satellites—the first European transmitter location system. *Int. J. Satell. Commun.*, **15**(4):155-183. [http://dx.doi.org/10.1002/\(SICI\)1099-1247\(199707/08\)15:4<155::AID-SAT577>3.0.CO;2-U](http://dx.doi.org/10.1002/(SICI)1099-1247(199707/08)15:4<155::AID-SAT577>3.0.CO;2-U)
- Ho, K.C., Xu, W.W., 2004. An accurate algebraic solution for moving source location using TDOA and FDOA measurements. *IEEE Trans. Signal Process.*, **52**(9):2453-2463. <http://dx.doi.org/10.1109/TSP.2004.831921>
- Ho, K.C., Yang, L., 2008. On the use of a calibration emitter for source localization in the presence of sensor position uncertainty. *IEEE Trans. Signal Process.*, **56**(12):5758-5772. <http://dx.doi.org/10.1109/TSP.2008.929870>
- Ho, K.C., Lu, X.N., Kovavisaruch, L., 2007. Source localization using TDOA and FDOA measurements in the presence of receiver location errors: analysis and solution. *IEEE Trans. Signal Process.*, **55**(2):684-696. <http://dx.doi.org/10.1109/TSP.2006.885744>
- Ho, K.C., Chan, Y.T., 1993. Solution and performance analysis of geolocation by TDOA. *IEEE Trans. Aerosp. Electron. Syst.*, **29**(4):1311-1322. <http://dx.doi.org/10.1109/7.259534>
- Ho, K.C., Chan, Y.T., 1997. Geolocation of a known altitude

- object from TDOA and FDOA measurements. *IEEE Trans. Aerosp. Electron. Syst.*, **33**(3):770-783.  
<http://dx.doi.org/10.1109/7.599239>
- Huang, Y., Benesty, J., Elko, G.W., et al., 2001. Real-time passive source localization: a practical linear-correction least-squares approach. *IEEE Trans. Speech Audio Process.*, **9**(8):943-956. <http://dx.doi.org/10.1109/89.966097>
- Kovavisaruch, L., Ho, K.C., 2005. Modified Taylor-series method for source and receiver localization using TDOA measurements with erroneous receiver positions. Proc. IEEE Int. Symp. on Circuits and Systems, p.2295-2298.  
<http://dx.doi.org/10.1109/ISCAS.2005.1465082>
- Lee, K.E., Ahn, D.M., Lee, Y.J., et al., 2000. A total squares algorithm for the source location estimation using GEO satellites. Proc. 21st Century Military Communications Conf., p.271-275.  
<http://dx.doi.org/10.1109/MILCOM.2000.904954>
- Lu, X.N., Ho, K.C., 2006a. Taylor-series technique for source localization using AOAs in the presence of sensor location errors. Proc. 4th IEEE Workshop on Sensor Array and Multichannel Processing, p.190-194.  
<http://dx.doi.org/10.1109/SAM.2006.1706119>
- Lu, X.N., Ho, K.C., 2006b. Analysis of the degradation in source location accuracy in the presence of sensor location error. Proc. IEEE Int. Conf. on Acoustics, Speech and Signal Processing, p.925-928.  
<http://dx.doi.org/10.1109/ICASSP.2006.1661121>
- Marzetta, T.L., 1993. A simple derivation of the constrained multiple parameter Cramer-Rao bound. *IEEE Trans. Acoust. Speech Signal Process.*, **41**(6):2247-2249.  
<http://dx.doi.org/10.1109/78.218151>
- Mason, J., 2004. Algebraic two-satellite TOA/FOA position solution on an ellipsoidal Earth. *IEEE Trans. Aerosp. Electron. Syst.*, **40**(3):1087-1092.  
<http://dx.doi.org/10.1109/TAES.2004.1337476>
- Mušicki, D., Koch, W., 2008. Geolocation using TDOA and FDOA measurements. Proc. 11th IEEE Int. Conf. on Information Fusion, p.1-8.
- Mušicki, D., Kaune, R., Koch, W., 2010. Mobile emitter geolocation and tracking using TDOA and FDOA measurements. *IEEE Trans. Signal Process.*, **58**(3):1863-1874.  
<http://dx.doi.org/10.1109/TSP.2009.2037075>
- Niezwoda, G.H., Ho, K.C., 1994. Geolocation by combined range difference and range rate difference measurements. Proc. IEEE Int. Conf. on Acoustics, Speech and Signal Processing, p.357-360.  
<http://dx.doi.org/10.1109/ICASSP.1994.389616>
- Pattison, T., Chou, S.I., 2000. Sensitivity analysis of dual-satellite geolocation. *IEEE Trans. Aerosp. Electron. Syst.*, **36**(1):56-71. <http://dx.doi.org/10.1109/7.826312>
- Witzgall, H., 2014. Ground vehicle Doppler geolocation. Proc. IEEE Int. Conf. on Aerospace, p.1-8.  
<http://dx.doi.org/10.1109/AERO.2014.6836173>
- Wu, S.L., Luo, J.Q., 2009. Influence of position error on TDOA and FDOA measuring of dual-satellite passive location system. Proc. 3rd IEEE Int. Symp. on Microwave, Antenna, Propagation and EMC Technologies for Wireless Communications, p.293-296.  
<http://dx.doi.org/10.1109/MAPE.2009.5355928>
- Yang, K., An, J.P., Bu, X.Y., et al., 2010. Constrained total least-squares location algorithm using time-difference-of-arrival measurements. *IEEE Trans. Veh. Technol.*, **59**(3):1558-1562.  
<http://dx.doi.org/10.1109/TVT.2009.2037509>
- Yang, K.H., Jiang, L.Z., Luo, Z.Q., 2011. Efficient semidefinite relaxation for robust geolocation of unknown emitter by a satellite cluster using TDOA and FDOA measurements. Proc. IEEE Int. Conf. on Acoustics, Speech and Signal Processing, p.2584-2587.  
<http://dx.doi.org/10.1109/ICASSP.2011.5947013>
- Yang, L., Ho, K.C., 2010a. On using multiple calibration emitters and their geometric effects for removing sensor position errors in TDOA localization. Proc. IEEE Int. Conf. on Acoustics, Speech and Signal Processing, p.14-19.  
<http://dx.doi.org/10.1109/ICASSP.2010.5496241>
- Yang, L., Ho, K.C., 2010b. Alleviating sensor position error in source localization using calibration emitters at inaccurate locations. *IEEE Trans. Signal Process.*, **58**(1):67-83.  
<http://dx.doi.org/10.1109/TSP.2009.2028947>
- Yu, H., Huang, G., Gao, J., 2012. Constrained total least-squares localization algorithm using time difference of arrival and frequency difference of arrival measurements with sensor location uncertainties. *IET Radar Sonar Navig.*, **6**(9):891-899.  
<http://dx.doi.org/10.1049/iet-rsn.2011.0205>

## Appendix A: Proof of Theorem 1

If  $A^{1/2}$  denotes the square root factor of  $A$ , i.e.,  $A=A^{1/2}A^{1/2}$ , then the proof of Eq. (1) is equivalent to verifying the following relationship:

$$\begin{aligned} I_n - \frac{A^{1/2}bb^T A^{1/2}}{b^T Ab} \\ = A^{-1/2}\Phi(b)(\Phi^T(b)A^{-1}\Phi(b))^{-1}\Phi^T(b)A^{-1/2}. \end{aligned} \quad (A1)$$

The left-hand side of Eq. (A1) can be rewritten as

$$\begin{aligned} I_n - \frac{A^{1/2}bb^T A^{1/2}}{b^T Ab} \\ = I_n - (A^{1/2}b)((A^{1/2}b)^T(A^{1/2}b))^{-1}(A^{1/2}b)^T \\ = \Pi^\perp(A^{1/2}b), \end{aligned} \quad (A2)$$

and the right-hand side of Eq. (A1) can be reformulated by

$$\begin{aligned} A^{-1/2}\Phi(b)(\Phi^T(b)A^{-1}\Phi(b))^{-1}\Phi^T(b)A^{-1/2} \\ = (A^{-1/2}\Phi(b))((A^{-1/2}\Phi(b))^T(A^{-1/2}\Phi(b)))^{-1} \\ \cdot (A^{-1/2}\Phi(b))^T = \Pi(A^{-1/2}\Phi(b)). \end{aligned} \quad (A3)$$

Also, according to the construction of matrix  $\Phi(\mathbf{b})$ , the following results hold:

$$\begin{cases} \text{(I) } \text{rank}[A^{-1/2}\Phi(\mathbf{b})] = \text{rank}[\Phi(\mathbf{b})] = n-1, \\ \text{(II) } (A^{1/2}\mathbf{b})^T(A^{-1/2}\Phi(\mathbf{b})) = \mathbf{b}^T\Phi(\mathbf{b}) = \mathbf{O}_{1 \times (n-1)}. \end{cases} \quad (\text{A4})$$

Using Eq. (A4) produces

$$\text{range}^\perp[A^{-1/2}\Phi(\mathbf{b})] = \text{range}[A^{1/2}\mathbf{b}], \quad (\text{A5})$$

which implies

$$\Pi^\perp(A^{1/2}\mathbf{b}) = \Pi(A^{-1/2}\Phi(\mathbf{b})). \quad (\text{A6})$$

Combining Eqs. (A2), (A3), and (A6), Theorem 1 holds true.

### Appendix B: Proof of Theorem 2

Analogous to the proof in Theorem 1, we should prove the following equality:

$$\begin{aligned} & I_{n+m} - \frac{A^{1/2}\mathbf{c}\mathbf{c}^T A^{1/2}}{\mathbf{c}^T \mathbf{A} \mathbf{c}} \\ &= A^{-1/2} \begin{bmatrix} \Phi(\mathbf{b}) & \mathbf{O}_{n \times m} \\ \mathbf{O}_{m \times (n-1)} & \mathbf{I}_m \end{bmatrix} \\ & \cdot \left( \begin{bmatrix} \Phi^T(\mathbf{b}) & \mathbf{O}_{(n-1) \times m} \\ \mathbf{O}_{m \times n} & \mathbf{I}_m \end{bmatrix} A^{-1} \begin{bmatrix} \Phi(\mathbf{b}) & \mathbf{O}_{n \times m} \\ \mathbf{O}_{m \times (n-1)} & \mathbf{I}_m \end{bmatrix} \right)^{-1} \\ & \cdot \begin{bmatrix} \Phi^T(\mathbf{b}) & \mathbf{O}_{(n-1) \times m} \\ \mathbf{O}_{m \times n} & \mathbf{I}_m \end{bmatrix} A^{-1/2}, \end{aligned} \quad (\text{B1})$$

where  $A^{1/2}$  is the square root factor of  $A$ . The left-hand side of Eq. (B1) can be represented as

$$\begin{aligned} & I_{n+m} - \frac{A^{1/2}\mathbf{c}\mathbf{c}^T A^{1/2}}{\mathbf{c}^T \mathbf{A} \mathbf{c}} \\ &= I_{n+m} - (A^{1/2}\mathbf{c})((A^{1/2}\mathbf{c})^T(A^{1/2}\mathbf{c}))^{-1}(A^{1/2}\mathbf{c})^T \\ &= \Pi^\perp(A^{1/2}\mathbf{c}), \end{aligned} \quad (\text{B2})$$

and the right-hand side of Eq. (B1) can be rewritten as Eq. (B3) (see page 1385).

Furthermore, with the definition of matrix  $\Phi(\mathbf{b})$  we obtain

$$\begin{cases} \text{(I) } \text{rank} \begin{bmatrix} A^{-1/2} \begin{bmatrix} \Phi(\mathbf{b}) & \mathbf{O}_{n \times m} \\ \mathbf{O}_{m \times (n-1)} & \mathbf{I}_m \end{bmatrix} \end{bmatrix} = n+m-1, \\ \text{(II) } (A^{1/2}\mathbf{c})^T \left( A^{-1/2} \begin{bmatrix} \Phi(\mathbf{b}) & \mathbf{O}_{n \times m} \\ \mathbf{O}_{m \times (n-1)} & \mathbf{I}_m \end{bmatrix} \right) \\ = [\mathbf{b}^T \ \mathbf{O}_{1 \times m}] \begin{bmatrix} \Phi(\mathbf{b}) & \mathbf{O}_{n \times m} \\ \mathbf{O}_{m \times (n-1)} & \mathbf{I}_m \end{bmatrix} \\ = [\mathbf{b}^T \Phi(\mathbf{b}) \ \mathbf{O}_{1 \times m}] = \mathbf{O}_{1 \times (n+m-1)}, \end{cases} \quad (\text{B4})$$

which yields the following result:

$$\text{range}^\perp \begin{bmatrix} A^{-1/2} \begin{bmatrix} \Phi(\mathbf{b}) & \mathbf{O}_{n \times m} \\ \mathbf{O}_{m \times (n-1)} & \mathbf{I}_m \end{bmatrix} \end{bmatrix} = \text{range}[A^{1/2}\mathbf{c}], \quad (\text{B5})$$

from which it can be verified that

$$\Pi^\perp(A^{1/2}\mathbf{c}) = \Pi \left( A^{-1/2} \begin{bmatrix} \Phi(\mathbf{b}) & \mathbf{O}_{n \times m} \\ \mathbf{O}_{m \times (n-1)} & \mathbf{I}_m \end{bmatrix} \right), \quad (\text{B6})$$

which combined with Eqs. (B2) and (B3) proves Theorem 2.

### Appendix C: Proof of Proposition 1

Applying Eq. (32) produces

$$\begin{aligned} & Z^{(b)} - Y^{(b)T} \Phi(Du^0) (\Phi^T(Du^0) X^{(b)} \Phi(Du^0))^{-1} \\ & \cdot \Phi^T(Du^0) Y^{(b)} = Q_2^{-1} + H_2^T(u^0, s^0) Q_1^{-1} H_2(u^0, s^0) \\ & - H_2^T(u^0, s^0) Q_1^{-1} H_1(u^0, s^0) \Phi(Du^0) \\ & \cdot (\Phi^T(Du^0) H_1^T(u^0, s^0) Q_1^{-1} H_1(u^0, s^0) \Phi(Du^0))^{-1} \\ & \cdot \Phi^T(Du^0) H_1^T(u^0, s^0) Q_1^{-1} H_2(u^0, s^0). \end{aligned} \quad (\text{C1})$$

In addition, it follows from Theorem 3 that

$$\begin{aligned} & H_2^T(u^0, s^0) Q_1^{-1} H_2(u^0, s^0) \\ & - H_2^T(u^0, s^0) Q_1^{-1} H_1(u^0, s^0) \Phi(Du^0) \\ & \cdot (\Phi^T(Du^0) H_1^T(u^0, s^0) Q_1^{-1} H_1(u^0, s^0) \Phi(Du^0))^{-1} \\ & \cdot \Phi^T(Du^0) H_1^T(u^0, s^0) Q_1^{-1} H_2(u^0, s^0) \geq \mathbf{O}, \end{aligned} \quad (\text{C2})$$

Combining inequality (C2) with Eq. (C1) yields

$$\begin{aligned} & Z^{(b)} - Y^{(b)T} \Phi(Du^0) \\ & \cdot (\Phi^T(Du^0) X^{(b)} \Phi(Du^0))^{-1} \Phi^T(Du^0) Y^{(b)} > \mathbf{O}. \end{aligned} \quad (\text{C3})$$

Then, the second term of the right hand side of the last equality in Eq. (37) is positive semidefinite because it

has a symmetric structure. As a consequence, we know that  $\text{CRB}^{(b)}(\mathbf{u}^0) \geq \text{CRB}^{(a)}(\mathbf{u}^0)$ , which completes the proof.

### Appendix D: Proof of Proposition 2

It follows immediately from the matrix inversion formula in Table 2 that

$$\begin{aligned} \tilde{\mathbf{Q}}_1^{-1} &= \mathbf{Q}_1^{-1} - \mathbf{Q}_1^{-1} \mathbf{H}_2(\mathbf{u}^0, \mathbf{s}^0) \\ &\quad \cdot (\mathbf{H}_2^T(\mathbf{u}^0, \mathbf{s}^0) \mathbf{Q}_1^{-1} \mathbf{H}_2(\mathbf{u}^0, \mathbf{s}^0) + \mathbf{Q}_2^{-1})^{-1} \\ &\quad \cdot \mathbf{H}_2^T(\mathbf{u}^0, \mathbf{s}^0) \mathbf{Q}_1^{-1}. \end{aligned} \quad (\text{D1})$$

The substitution of Eq. (D1) into the right-hand side of Eq. (40) produces Eq. (D2) (see page 1385), which proves Proposition 2.

### Appendix E: Proof of Proposition 3

It can be readily seen from Eqs. (32) and (38) that

$$\begin{aligned} &(\text{CRB}^{(b)}(\mathbf{s}^0))^{-1} \\ &= \mathbf{Q}_2^{-1} + \mathbf{H}_2^T(\mathbf{u}^0, \mathbf{s}^0) \mathbf{Q}_1^{-1} \mathbf{H}_2(\mathbf{u}^0, \mathbf{s}^0) \\ &\quad - \mathbf{H}_2^T(\mathbf{u}^0, \mathbf{s}^0) \mathbf{Q}_1^{-1} \mathbf{H}_1(\mathbf{u}^0, \mathbf{s}^0) \Phi(\mathbf{D}\mathbf{u}^0) \\ &\quad \cdot (\Phi^T(\mathbf{D}\mathbf{u}^0) \mathbf{H}_1^T(\mathbf{u}^0, \mathbf{s}^0) \mathbf{Q}_1^{-1} \mathbf{H}_1(\mathbf{u}^0, \mathbf{s}^0) \Phi(\mathbf{D}\mathbf{u}^0))^{-1} \\ &\quad \cdot \Phi^T(\mathbf{D}\mathbf{u}^0) \mathbf{H}_1^T(\mathbf{u}^0, \mathbf{s}^0) \mathbf{Q}_1^{-1} \mathbf{H}_2(\mathbf{u}^0, \mathbf{s}^0) \\ &= \mathbf{Q}_2^{-1} + \mathbf{H}_2^T(\mathbf{u}^0, \mathbf{s}^0) \mathbf{A} \mathbf{H}_2(\mathbf{u}^0, \mathbf{s}^0), \end{aligned} \quad (\text{E1})$$

where

$$\begin{aligned} \mathbf{A} &= \mathbf{Q}_1^{-1} - \mathbf{Q}_1^{-1} \mathbf{H}_1(\mathbf{u}^0, \mathbf{s}^0) \Phi(\mathbf{D}\mathbf{u}^0) \\ &\quad \cdot (\Phi^T(\mathbf{D}\mathbf{u}^0) \mathbf{H}_1^T(\mathbf{u}^0, \mathbf{s}^0) \mathbf{Q}_1^{-1} \mathbf{H}_1(\mathbf{u}^0, \mathbf{s}^0) \Phi(\mathbf{D}\mathbf{u}^0))^{-1} \\ &\quad \cdot \Phi^T(\mathbf{D}\mathbf{u}^0) \mathbf{H}_1^T(\mathbf{u}^0, \mathbf{s}^0) \mathbf{Q}_1^{-1}. \end{aligned} \quad (\text{E2})$$

Let  $\mathbf{Q}_1^{1/2}$  be the square root factor of  $\mathbf{Q}_1$ . Then, matrix  $\mathbf{A}$  can be reformulated as

$$\mathbf{A} = \mathbf{Q}_1^{-1/2} \Pi^\perp (\mathbf{Q}_1^{-1/2} \mathbf{H}_1(\mathbf{u}^0, \mathbf{s}^0) \Phi(\mathbf{D}\mathbf{u}^0)) \mathbf{Q}_1^{-1/2} \geq \mathbf{O}. \quad (\text{E3})$$

Inserting inequality (E3) back into Eq. (E1) leads to  $(\text{CRB}^{(b)}(\mathbf{s}^0))^{-1} \geq \mathbf{Q}_2^{-1}$ , which is equivalent to  $\text{CRB}^{(b)}(\mathbf{s}^0) \leq \mathbf{Q}_2$ .

Furthermore, when  $M=3$ ,  $\mathbf{H}_1(\mathbf{u}^0, \mathbf{s}^0) \Phi(\mathbf{D}\mathbf{u}^0)$  is an invertible square matrix of dimension 2, which combined with Eq. (E2) and yields

$$\begin{aligned} \mathbf{A} &= \mathbf{Q}_1^{-1/2} (\mathbf{I}_{M-1} - (\mathbf{Q}_1^{-1/2} \mathbf{H}_1(\mathbf{u}^0, \mathbf{s}^0) \Phi(\mathbf{D}\mathbf{u}^0)) \\ &\quad \cdot (\mathbf{Q}_1^{-1/2} \mathbf{H}_1(\mathbf{u}^0, \mathbf{s}^0) \Phi(\mathbf{D}\mathbf{u}^0))^{-1} \\ &\quad \cdot (\mathbf{Q}_1^{-1/2} \mathbf{H}_1(\mathbf{u}^0, \mathbf{s}^0) \Phi(\mathbf{D}\mathbf{u}^0))^{-T} \\ &\quad \cdot (\mathbf{Q}_1^{-1/2} \mathbf{H}_1(\mathbf{u}^0, \mathbf{s}^0) \Phi(\mathbf{D}\mathbf{u}^0))^T) \mathbf{Q}_1^{-1/2} \\ &= \mathbf{O}. \end{aligned} \quad (\text{E4})$$

Putting Eq. (E4) into Eq. (E1) leads to  $\text{CRB}^{(b)}(\mathbf{s}^0) = \mathbf{Q}_2$ . On the other hand, if  $\text{CRB}^{(b)}(\mathbf{s}^0) = \mathbf{Q}_2$ , then applying Eq. (E1) and the fact that  $\mathbf{H}_2(\mathbf{u}^0, \mathbf{s}^0)$  has a full row rank gives  $\mathbf{A} = \mathbf{O}$ . As a consequence, it can be directly observed from inequality (E3) that

$$\begin{aligned} \mathbf{I}_{M-1} &= \Pi (\mathbf{Q}_1^{-1/2} \mathbf{H}_1(\mathbf{u}^0, \mathbf{s}^0) \Phi(\mathbf{D}\mathbf{u}^0)) \\ &= (\mathbf{Q}_1^{-1/2} \mathbf{H}_1(\mathbf{u}^0, \mathbf{s}^0) \Phi(\mathbf{D}\mathbf{u}^0)) \\ &\quad \cdot ((\mathbf{Q}_1^{-1/2} \mathbf{H}_1(\mathbf{u}^0, \mathbf{s}^0) \Phi(\mathbf{D}\mathbf{u}^0))^T)^{-1} \\ &\quad \cdot (\mathbf{Q}_1^{-1/2} \mathbf{H}_1(\mathbf{u}^0, \mathbf{s}^0) \Phi(\mathbf{D}\mathbf{u}^0))^{-1} \\ &\quad \cdot (\mathbf{Q}_1^{-1/2} \mathbf{H}_1(\mathbf{u}^0, \mathbf{s}^0) \Phi(\mathbf{D}\mathbf{u}^0))^T, \end{aligned} \quad (\text{E5})$$

which implies that  $\mathbf{Q}_1^{-1/2} \mathbf{H}_1(\mathbf{u}^0, \mathbf{s}^0) \Phi(\mathbf{D}\mathbf{u}^0) \in \mathbb{R}^{(M-1) \times 2}$  is a square matrix of full rank. Hence,  $M=3$  holds. At this point, the proof of Proposition 3 is completed.

### Appendix F: Proof of Proposition 4

From Eq. (43), we obtain

$$\begin{aligned} \mathbf{X}^{(a)} &- (\mathbf{X}^{(c)} - \mathbf{Y}^{(c)} (\mathbf{Z}^{(c)})^{-1} \mathbf{Y}^{(c)T}) \\ &= \mathbf{Y}^{(c)} (\mathbf{Z}^{(c)})^{-1} \mathbf{Y}^{(c)T} \geq \mathbf{O}, \end{aligned} \quad (\text{F1})$$

which gives

$$\mathbf{X}^{(a)} \geq \mathbf{X}^{(c)} - \mathbf{Y}^{(c)} (\mathbf{Z}^{(c)})^{-1} \mathbf{Y}^{(c)T}. \quad (\text{F2})$$

Combining inequality (F2) and the fact that  $\Phi(\mathbf{D}\mathbf{u}^0)$  has full column rank leads to

$$\begin{aligned} &\Phi^T(\mathbf{D}\mathbf{u}^0) \mathbf{X}^{(a)} \Phi(\mathbf{D}\mathbf{u}^0) \\ &\geq \Phi^T(\mathbf{D}\mathbf{u}^0) (\mathbf{X}^{(c)} - \mathbf{Y}^{(c)} (\mathbf{Z}^{(c)})^{-1} \mathbf{Y}^{(c)T}) \Phi(\mathbf{D}\mathbf{u}^0), \end{aligned} \quad (\text{F3})$$

which is equivalent to

$$\begin{aligned} &[\Phi^T(\mathbf{D}\mathbf{u}^0) (\mathbf{X}^{(c)} - \mathbf{Y}^{(c)} (\mathbf{Z}^{(c)})^{-1} \mathbf{Y}^{(c)T}) \Phi(\mathbf{D}\mathbf{u}^0)]^{-1} \\ &\geq (\Phi^T(\mathbf{D}\mathbf{u}^0) \mathbf{X}^{(a)} \Phi(\mathbf{D}\mathbf{u}^0))^{-1}. \end{aligned} \quad (\text{F4})$$

Consequently, we arrive at



$$\begin{aligned} \mathbf{CRB}^{(c)}(\mathbf{u}^0) &= \Phi(\mathbf{D}\mathbf{u}^0) \\ & \cdot [\Phi^T(\mathbf{D}\mathbf{u}^0)(\mathbf{X}^{(c)} - \mathbf{Y}^{(c)}(\mathbf{Z}^{(c)})^{-1}\mathbf{Y}^{(c)T})\Phi(\mathbf{D}\mathbf{u}^0)]^{-1} \\ & \cdot \Phi^T(\mathbf{D}\mathbf{u}^0) \geq \Phi(\mathbf{D}\mathbf{u}^0)(\Phi^T(\mathbf{D}\mathbf{u}^0)\mathbf{X}^{(a)}\Phi(\mathbf{D}\mathbf{u}^0))^{-1} \\ & \cdot \Phi^T(\mathbf{D}\mathbf{u}^0) = \mathbf{CRB}^{(a)}(\mathbf{u}^0). \end{aligned} \quad (\text{F5})$$

Also, it can be seen from Eq. (43) and the matrix inversion formula in Table 2 that

$$\begin{aligned} & (\mathbf{X}^{(c)} - \mathbf{Y}^{(c)}(\mathbf{Z}^{(c)})^{-1}\mathbf{Y}^{(c)T}) \\ & - (\mathbf{X}^{(b)} - \mathbf{Y}^{(b)}(\mathbf{Z}^{(b)})^{-1}\mathbf{Y}^{(b)T}) \\ & = \mathbf{Y}^{(c)}((\mathbf{Z}^{(b)})^{-1} - (\mathbf{Z}^{(c)})^{-1})\mathbf{Y}^{(c)T} \\ & = \mathbf{Y}^{(c)}(\mathbf{Z}^{(b)})^{-1}\mathbf{G}_2^T(\mathbf{v}^0, \mathbf{s}^0) \cdot \\ & (\mathbf{P}_1 + \mathbf{G}_2(\mathbf{v}^0, \mathbf{s}^0)(\mathbf{Z}^{(b)})^{-1}\mathbf{G}_2^T(\mathbf{v}^0, \mathbf{s}^0))^{-1} \\ & \cdot \mathbf{G}_2(\mathbf{v}^0, \mathbf{s}^0)(\mathbf{Z}^{(b)})^{-1}\mathbf{Y}^{(c)T} \geq \mathbf{O}. \end{aligned} \quad (\text{F6})$$

Combining inequality (F6) and the fact that  $\Phi(\mathbf{D}\mathbf{u}^0)$  has a full column rank leads to

$$\begin{aligned} & \Phi^T(\mathbf{D}\mathbf{u}^0)(\mathbf{X}^{(c)} - \mathbf{Y}^{(c)}(\mathbf{Z}^{(c)})^{-1}\mathbf{Y}^{(c)T})\Phi(\mathbf{D}\mathbf{u}^0) \\ & \geq \Phi^T(\mathbf{D}\mathbf{u}^0)(\mathbf{X}^{(b)} - \mathbf{Y}^{(b)}(\mathbf{Z}^{(b)})^{-1}\mathbf{Y}^{(b)T})\Phi(\mathbf{D}\mathbf{u}^0), \end{aligned} \quad (\text{F7})$$

which is equivalent to

$$\begin{aligned} & [\Phi^T(\mathbf{D}\mathbf{u}^0)(\mathbf{X}^{(b)} - \mathbf{Y}^{(b)}(\mathbf{Z}^{(b)})^{-1}\mathbf{Y}^{(b)T})\Phi(\mathbf{D}\mathbf{u}^0)]^{-1} \\ & \geq [\Phi^T(\mathbf{D}\mathbf{u}^0)(\mathbf{X}^{(c)} - \mathbf{Y}^{(c)}(\mathbf{Z}^{(c)})^{-1}\mathbf{Y}^{(c)T})\Phi(\mathbf{D}\mathbf{u}^0)]^{-1}. \end{aligned} \quad (\text{F8})$$

Then, we obtain

$$\begin{aligned} \mathbf{CRB}^{(b)}(\mathbf{u}^0) &= \Phi(\mathbf{D}\mathbf{u}^0) \\ & \cdot [\Phi^T(\mathbf{D}\mathbf{u}^0)(\mathbf{X}^{(b)} - \mathbf{Y}^{(b)}(\mathbf{Z}^{(b)})^{-1}\mathbf{Y}^{(b)T})\Phi(\mathbf{D}\mathbf{u}^0)]^{-1} \\ & \cdot \Phi^T(\mathbf{D}\mathbf{u}^0) \geq \Phi(\mathbf{D}\mathbf{u}^0) \\ & \cdot [\Phi^T(\mathbf{D}\mathbf{u}^0)(\mathbf{X}^{(c)} - \mathbf{Y}^{(c)}(\mathbf{Z}^{(c)})^{-1}\mathbf{Y}^{(c)T})\Phi(\mathbf{D}\mathbf{u}^0)]^{-1} \\ & \cdot \Phi^T(\mathbf{D}\mathbf{u}^0) = \mathbf{CRB}^{(c)}(\mathbf{u}^0). \end{aligned} \quad (\text{F9})$$

Combining inequality (F9) with Eq. (F5) completes the proof.

## Appendix G: Proof of Proposition 5

Mathematically, to reduce  $\mathbf{CRB}^{(c)}(\mathbf{u}^0)$  back to  $\mathbf{CRB}^{(a)}(\mathbf{u}^0)$ , the second term on the right-hand side of the last equality in Eq. (48) must approach zero, which is equivalent to proving

$$\begin{aligned} \mathbf{Z}^{(c)} &= \mathbf{H}_2^T(\mathbf{u}^0, \mathbf{s}^0)\mathbf{Q}_1^{-1}\mathbf{H}_2(\mathbf{u}^0, \mathbf{s}^0) \\ & + \mathbf{Q}_2^{-1} + \mathbf{G}_2^T(\mathbf{v}^0, \mathbf{s}^0)\mathbf{P}_1^{-1}\mathbf{G}_2(\mathbf{v}^0, \mathbf{s}^0) \rightarrow \infty. \end{aligned} \quad (\text{G1})$$

Indeed, when  $\mathbf{G}_2(\mathbf{v}^0, \mathbf{s}^0)$  has a full column rank and  $\mathbf{P}_1$  is near zero,  $\mathbf{G}_2^T(\mathbf{v}^0, \mathbf{s}^0)\mathbf{P}_1^{-1}\mathbf{G}_2(\mathbf{v}^0, \mathbf{s}^0)$  tends to infinity, which leads to  $\mathbf{Z}^{(c)} \rightarrow \infty$ . Then, Proposition 5 holds true.

## Appendix H: Proof of Proposition 7

In light of the results in Proposition 4, we need only to prove  $\mathbf{CRB}^{(d)}(\mathbf{u}^0) \geq \mathbf{CRB}^{(c)}(\mathbf{u}^0)$  and  $\mathbf{CRB}^{(b)}(\mathbf{u}^0) \geq \mathbf{CRB}^{(d)}(\mathbf{u}^0)$ .

First, applying the matrix inversion formula in Table 2 yields Eq. (H1), and  $\mathbf{A}$  in Eq. (H1) is stated in Eq. (H2). Inserting Eq. (52) into Eq. (H2) produces Eq. (H3). Eqs. (H1)–(H3) are shown on page 1385.

In Eq. (H3) the last equality holds because of the matrix inversion formula in Table 2. From Eq. (H3), it follows that  $\mathbf{A} > \mathbf{O}$  or, equivalently,  $\mathbf{A}^{-1} > \mathbf{O}$ . Combining Eqs. (48), (57), and (H1) leads to Eq. (H4) (see page 1385).

The term on the right-hand side of Eq. (H4) is the increase in CRB due to calibration source position errors. It is positive semidefinite, because it has a symmetric structure and  $\mathbf{A}^{-1}$  is positive definite. As a result,  $\mathbf{CRB}^{(d)}(\mathbf{u}^0) \geq \mathbf{CRB}^{(c)}(\mathbf{u}^0)$  holds true.

Second, it can be seen from Eq. (52) and the matrix inversion formula in Table 2 that

$$\begin{aligned} & \mathbf{Z}^{(d)} - \mathbf{W}^{(d)T}(\mathbf{T}^{(d)})^{-1}\mathbf{W}^{(d)} \\ & = \mathbf{Z}^{(b)} + \mathbf{G}_2^T(\mathbf{v}^0, \mathbf{s}^0) \\ & \cdot \mathbf{P}_1^{-1}\mathbf{G}_2(\mathbf{v}^0, \mathbf{s}^0) - \mathbf{G}_2^T(\mathbf{v}^0, \mathbf{s}^0)\mathbf{P}_1^{-1}\mathbf{G}_1(\mathbf{v}^0, \mathbf{s}^0) \\ & \cdot (\mathbf{G}_1^T(\mathbf{v}^0, \mathbf{s}^0)\mathbf{P}_1^{-1}\mathbf{G}_1(\mathbf{v}^0, \mathbf{s}^0) + \mathbf{P}_2^{-1})^{-1} \\ & \cdot \mathbf{G}_1^T(\mathbf{v}^0, \mathbf{s}^0)\mathbf{P}_1^{-1}\mathbf{G}_2(\mathbf{v}^0, \mathbf{s}^0) \\ & = \mathbf{Z}^{(b)} + \mathbf{G}_2^T(\mathbf{v}^0, \mathbf{s}^0)(\mathbf{P}_1 + \mathbf{G}_1(\mathbf{v}^0, \mathbf{s}^0)\mathbf{P}_2\mathbf{G}_1^T(\mathbf{v}^0, \mathbf{s}^0))^{-1} \\ & \cdot \mathbf{G}_2(\mathbf{v}^0, \mathbf{s}^0). \end{aligned} \quad (\text{H5})$$

Applying the matrix inversion formula in Table 2 again yields Eq. (H6) (see page 1385), where

$$\begin{aligned} \mathbf{B} &= \mathbf{P}_1 + \mathbf{G}_1(\mathbf{v}^0, \mathbf{s}^0)\mathbf{P}_2\mathbf{G}_1^T(\mathbf{v}^0, \mathbf{s}^0) + \mathbf{G}_2(\mathbf{v}^0, \mathbf{s}^0) \\ & \cdot (\mathbf{Z}^{(b)} - \mathbf{Y}^{(b)T}\Phi(\mathbf{D}\mathbf{u}^0)(\Phi^T(\mathbf{D}\mathbf{u}^0)\mathbf{X}^{(b)}\Phi(\mathbf{D}\mathbf{u}^0))^{-1} \\ & \cdot \Phi^T(\mathbf{D}\mathbf{u}^0)\mathbf{Y}^{(b)})^{-1}\mathbf{G}_2^T(\mathbf{v}^0, \mathbf{s}^0). \end{aligned} \quad (\text{H7})$$

It is straightforward to verify that  $\mathbf{B} > \mathbf{O}$  or, equivalently,  $\mathbf{B}^{-1} > \mathbf{O}$ . Combining Eqs. (37), (57), and (H7) produces

$$\begin{aligned}
& A^{-1/2} \begin{bmatrix} \Phi(\mathbf{b}) & \mathbf{O}_{n \times m} \\ \mathbf{O}_{m \times (n-1)} & \mathbf{I}_m \end{bmatrix} \left( \begin{bmatrix} \Phi^T(\mathbf{b}) & \mathbf{O}_{(n-1) \times m} \\ \mathbf{O}_{m \times n} & \mathbf{I}_m \end{bmatrix} A^{-1} \begin{bmatrix} \Phi(\mathbf{b}) & \mathbf{O}_{n \times m} \\ \mathbf{O}_{m \times (n-1)} & \mathbf{I}_m \end{bmatrix} \right)^{-1} \begin{bmatrix} \Phi^T(\mathbf{b}) & \mathbf{O}_{(n-1) \times m} \\ \mathbf{O}_{m \times n} & \mathbf{I}_m \end{bmatrix} A^{-1/2} \\
&= \left( A^{-1/2} \begin{bmatrix} \Phi(\mathbf{b}) & \mathbf{O}_{n \times m} \\ \mathbf{O}_{m \times (n-1)} & \mathbf{I}_m \end{bmatrix} \right) \left( \left( A^{-1/2} \begin{bmatrix} \Phi(\mathbf{b}) & \mathbf{O}_{n \times m} \\ \mathbf{O}_{m \times (n-1)} & \mathbf{I}_m \end{bmatrix} \right)^T \left( A^{-1/2} \begin{bmatrix} \Phi(\mathbf{b}) & \mathbf{O}_{n \times m} \\ \mathbf{O}_{m \times (n-1)} & \mathbf{I}_m \end{bmatrix} \right) \right)^{-1} \\
&\cdot \left( A^{-1/2} \begin{bmatrix} \Phi(\mathbf{b}) & \mathbf{O}_{n \times m} \\ \mathbf{O}_{m \times (n-1)} & \mathbf{I}_m \end{bmatrix} \right)^T = \Pi \left( A^{-1/2} \begin{bmatrix} \Phi(\mathbf{b}) & \mathbf{O}_{n \times m} \\ \mathbf{O}_{m \times (n-1)} & \mathbf{I}_m \end{bmatrix} \right). \tag{B3}
\end{aligned}$$

$$\begin{aligned}
& \Phi(D\mathbf{u}^0) (\Phi^T(D\mathbf{u}^0) H_1^T(\mathbf{u}^0, \mathbf{s}^0) \tilde{\mathcal{Q}}_1^{-1} H_1(\mathbf{u}^0, \mathbf{s}^0) \Phi(D\mathbf{u}^0))^{-1} \Phi^T(D\mathbf{u}^0) \\
&= \Phi(D\mathbf{u}^0) \{ \Phi^T(D\mathbf{u}^0) [H_1^T(\mathbf{u}^0, \mathbf{s}^0) \tilde{\mathcal{Q}}_1^{-1} H_1(\mathbf{u}^0, \mathbf{s}^0) - H_1^T(\mathbf{u}^0, \mathbf{s}^0) \tilde{\mathcal{Q}}_1^{-1} H_2(\mathbf{u}^0, \mathbf{s}^0) \\
&\quad \cdot (H_2^T(\mathbf{u}^0, \mathbf{s}^0) \tilde{\mathcal{Q}}_1^{-1} H_2(\mathbf{u}^0, \mathbf{s}^0) + \tilde{\mathcal{Q}}_2^{-1})^{-1} H_2^T(\mathbf{u}^0, \mathbf{s}^0) \tilde{\mathcal{Q}}_1^{-1} H_1(\mathbf{u}^0, \mathbf{s}^0)] \Phi(D\mathbf{u}^0) \}^{-1} \Phi^T(D\mathbf{u}^0) \\
&= \Phi(D\mathbf{u}^0) (\Phi^T(D\mathbf{u}^0) (X^{(b)} - Y^{(b)} (Z^{(b)})^{-1} Y^{(b)T}) \Phi(D\mathbf{u}^0))^{-1} \Phi^T(D\mathbf{u}^0) \\
&= \text{CRB}^{(b)}(\mathbf{u}^0). \tag{D2}
\end{aligned}$$

$$\begin{aligned}
& (Z^{(d)} - Y^{(d)T} \Phi(D\mathbf{u}^0) (\Phi^T(D\mathbf{u}^0) X^{(d)} \Phi(D\mathbf{u}^0))^{-1} \Phi^T(D\mathbf{u}^0) Y^{(d)} - W^{(d)T} (T^{(d)})^{-1} W^{(d)})^{-1} \\
&= (Z^{(d)} - Y^{(d)T} \Phi(D\mathbf{u}^0) (\Phi^T(D\mathbf{u}^0) X^{(d)} \Phi(D\mathbf{u}^0))^{-1} \Phi^T(D\mathbf{u}^0) Y^{(d)})^{-1} \\
&\quad + (Z^{(d)} - Y^{(d)T} \Phi(D\mathbf{u}^0) (\Phi^T(D\mathbf{u}^0) X^{(d)} \Phi(D\mathbf{u}^0))^{-1} \Phi^T(D\mathbf{u}^0) Y^{(d)})^{-1} W^{(d)T} \\
&\quad \cdot A^{-1} W^{(d)} (Z^{(d)} - Y^{(d)T} \Phi(D\mathbf{u}^0) (\Phi^T(D\mathbf{u}^0) X^{(d)} \Phi(D\mathbf{u}^0))^{-1} \Phi^T(D\mathbf{u}^0) Y^{(d)})^{-1}. \tag{H1}
\end{aligned}$$

$$A = T^{(d)} - W^{(d)} (Z^{(d)} - Y^{(d)T} \Phi(D\mathbf{u}^0) (\Phi^T(D\mathbf{u}^0) X^{(d)} \Phi(D\mathbf{u}^0))^{-1} \Phi^T(D\mathbf{u}^0) Y^{(d)})^{-1} W^{(d)T}. \tag{H2}$$

$$\begin{aligned}
& A = P_2^{-1} + G_1^T(\mathbf{v}^0, \mathbf{s}^0) \\
&\quad \cdot [P_1^{-1} - P_1^{-1} G_2(\mathbf{v}^0, \mathbf{s}^0) (Z^{(d)} - Y^{(d)T} \Phi(D\mathbf{u}^0) (\Phi^T(D\mathbf{u}^0) X^{(d)} \Phi(D\mathbf{u}^0))^{-1} \\
&\quad \cdot \Phi^T(D\mathbf{u}^0) Y^{(d)})^{-1} G_2^T(\mathbf{v}^0, \mathbf{s}^0) P_1^{-1}] G_1(\mathbf{v}^0, \mathbf{s}^0) \\
&= P_2^{-1} + G_1^T(\mathbf{v}^0, \mathbf{s}^0) [P_1 + G_2(\mathbf{v}^0, \mathbf{s}^0) (Z^{(b)} - Y^{(b)T} \Phi(D\mathbf{u}^0) (\Phi^T(D\mathbf{u}^0) X^{(b)} \Phi(D\mathbf{u}^0))^{-1} \\
&\quad \cdot \Phi^T(D\mathbf{u}^0) Y^{(b)})^{-1} G_2^T(\mathbf{v}^0, \mathbf{s}^0)]^{-1} G_1(\mathbf{v}^0, \mathbf{s}^0). \tag{H3}
\end{aligned}$$

$$\begin{aligned}
& \text{CRB}^{(d)}(\mathbf{u}^0) - \text{CRB}^{(c)}(\mathbf{u}^0) \\
&= \Phi(D\mathbf{u}^0) (\Phi^T(D\mathbf{u}^0) X^{(d)} \Phi(D\mathbf{u}^0))^{-1} \Phi^T(D\mathbf{u}^0) Y^{(d)} \\
&\quad \cdot (Z^{(d)} - Y^{(d)T} \Phi(D\mathbf{u}^0) (\Phi^T(D\mathbf{u}^0) X^{(d)} \Phi(D\mathbf{u}^0))^{-1} \\
&\quad \cdot \Phi^T(D\mathbf{u}^0) Y^{(d)})^{-1} W^{(d)T} A^{-1} W^{(d)} (Z^{(d)} - Y^{(d)T} \Phi(D\mathbf{u}^0) (\Phi^T(D\mathbf{u}^0) X^{(d)} \Phi(D\mathbf{u}^0))^{-1} \\
&\quad \cdot \Phi^T(D\mathbf{u}^0) Y^{(d)})^{-1} Y^{(d)T} \Phi(D\mathbf{u}^0) (\Phi^T(D\mathbf{u}^0) X^{(d)} \Phi(D\mathbf{u}^0))^{-1} \Phi^T(D\mathbf{u}^0). \tag{H4}
\end{aligned}$$

$$\begin{aligned}
& (Z^{(d)} - Y^{(d)T} \Phi(D\mathbf{u}^0) (\Phi^T(D\mathbf{u}^0) X^{(d)} \Phi(D\mathbf{u}^0))^{-1} \Phi^T(D\mathbf{u}^0) Y^{(d)} - W^{(d)T} (T^{(d)})^{-1} W^{(d)})^{-1} \\
&= (Z^{(b)} - Y^{(b)T} \Phi(D\mathbf{u}^0) (\Phi^T(D\mathbf{u}^0) X^{(b)} \Phi(D\mathbf{u}^0))^{-1} \Phi^T(D\mathbf{u}^0) Y^{(b)})^{-1} \\
&\quad - (Z^{(b)} - Y^{(b)T} \Phi(D\mathbf{u}^0) (\Phi^T(D\mathbf{u}^0) X^{(b)} \Phi(D\mathbf{u}^0))^{-1} \Phi^T(D\mathbf{u}^0) Y^{(b)})^{-1} G_2^T(\mathbf{v}^0, \mathbf{s}^0) \\
&\quad \cdot B^{-1} G_2(\mathbf{v}^0, \mathbf{s}^0) (Z^{(b)} - Y^{(b)T} \Phi(D\mathbf{u}^0) (\Phi^T(D\mathbf{u}^0) X^{(b)} \Phi(D\mathbf{u}^0))^{-1} \Phi^T(D\mathbf{u}^0) Y^{(b)})^{-1}. \tag{H6}
\end{aligned}$$

$$\begin{aligned}
 & \text{CRB}^{(b)}(u^0) - \text{CRB}^{(d)}(u^0) \\
 &= \Phi(Du^0)(\Phi^T(Du^0)X^{(b)}\Phi(Du^0))^{-1}\Phi^T(Du^0)Y^{(b)} \\
 & \cdot (Z^{(b)} - Y^{(b)T}\Phi(Du^0)(\Phi^T(Du^0)X^{(b)}\Phi(Du^0))^{-1} \\
 & \cdot \Phi^T(Du^0)Y^{(b)})^{-1}G_2^T(v^0, s^0)B^{-1}G_2(v^0, s^0) \\
 & \cdot (Z^{(b)} - Y^{(b)T}\Phi(Du^0)(\Phi^T(Du^0)X^{(b)}\Phi(Du^0))^{-1} \\
 & \cdot \Phi^T(Du^0)Y^{(b)})Y^{(b)T-1}\Phi(Du^0) \\
 & \cdot (\Phi^T(Du^0)X^{(b)}\Phi(Du^0))^{-1}\Phi^T(Du^0).
 \end{aligned} \tag{H8}$$

The term on the right-hand side of Eq. (H8) is the performance improvement due to the introduction of the calibration sources, although their positions are not known exactly. It is positive semidefinite because it has a symmetric structure and  $B^{-1}$  is positive definite. As a consequence,  $\text{CRB}^{(b)}(u^0) \geq \text{CRB}^{(d)}(u^0)$  holds true. At this point, the proof of Proposition 7 is complete.

### Appendix I: Proof of Proposition 10

It can be readily seen from Eqs. (52) and (59) that

$$\begin{aligned}
 & (\text{CRB}^{(d)}(v^0))^{-1} \\
 &= P_2^{-1} + G_1^T(v^0, s^0)P_1^{-1}G_1(v^0, s^0) \\
 & \quad - G_1^T(v^0, s^0)P_1^{-1}G_2(v^0, s^0) \\
 & \quad \cdot (G_2^T(v^0, s^0)P_1^{-1}G_2(v^0, s^0) + Q_2^{-1} \\
 & \quad + H_2^T(u^0, s^0)Q_1^{-1}H_2(u^0, s^0) - H_2^T(u^0, s^0)Q_1^{-1} \\
 & \quad \cdot H_1(u^0, s^0)\Phi(Du^0)(\Phi^T(Du^0)H_1^T(u^0, s^0)Q_1^{-1} \\
 & \quad \cdot H_1(u^0, s^0)\Phi(Du^0))^{-1}\Phi^T(Du^0)H_1^T(u^0, s^0)Q_1^{-1} \\
 & \quad \cdot H_2(u^0, s^0))^{-1}G_2^T(v^0, s^0)P_1^{-1}G_1(v^0, s^0),
 \end{aligned} \tag{I1}$$

from which  $(\text{CRB}^{(d)}(v^0))^{-1}$  can be rewritten as

$$\begin{aligned}
 & (\text{CRB}^{(d)}(v^0))^{-1} \\
 &= P_2^{-1} + G_1^T(v^0, s^0)P_1^{-1}G_1(v^0, s^0) - G_1^T(v^0, s^0)P_1^{-1}G_2(v^0, s^0) \\
 & \quad \cdot (G_2^T(v^0, s^0)P_1^{-1}G_2(v^0, s^0) + Q_2^{-1} + H_2^T(u^0, s^0) \\
 & \quad \cdot Q_1^{-1/2}\Pi^\perp(Q_1^{-1/2}H_1(u^0, s^0)\Phi(Du^0)) \\
 & \quad \cdot Q_1^{-1/2}H_2(u^0, s^0))^{-1} \\
 & \quad \cdot G_2^T(v^0, s^0)P_1^{-1}G_1(v^0, s^0),
 \end{aligned} \tag{I2}$$

which implies that

$$\begin{aligned}
 & (\text{CRB}^{(d)}(v^0))^{-1} \geq P_2^{-1} + G_1^T(v^0, s^0)P_1^{-1}G_1(v^0, s^0) \\
 & \quad - G_1^T(v^0, s^0)P_1^{-1}G_2(v^0, s^0) \\
 & \quad \cdot (G_2^T(v^0, s^0)P_1^{-1}G_2(v^0, s^0) + Q_2^{-1})^{-1} \\
 & \quad \cdot G_2^T(v^0, s^0)P_1^{-1}G_1(v^0, s^0).
 \end{aligned} \tag{I3}$$

In addition, using the matrix inversion formula in Table 2 yields

$$\begin{aligned}
 & (P_1 + G_2(v^0, s^0)Q_2G_2^T(v^0, s^0))^{-1} \\
 &= P_1^{-1} - P_1^{-1}G_2(v^0, s^0) \\
 & \quad \cdot (G_2^T(v^0, s^0)P_1^{-1}G_2(v^0, s^0) + Q_2^{-1})^{-1}G_2^T(v^0, s^0)P_1^{-1}.
 \end{aligned} \tag{I4}$$

Combining Eq. (I4) with Eq. (I3) yields

$$\begin{aligned}
 & (\text{CRB}^{(d)}(v^0))^{-1} \geq P_2^{-1} + G_1^T(v^0, s^0)(P_1 + G_2(v^0, s^0) \\
 & \quad \cdot Q_2G_2^T(v^0, s^0))^{-1}G_1(v^0, s^0) \\
 & \geq P_2^{-1} \Leftrightarrow \text{CRB}^{(d)}(v^0) \leq P_2.
 \end{aligned} \tag{I5}$$

Then, Proposition 10 is proved.

### Appendix J: Proof of Proposition 11

Substituting Eq. (28) into Eq. (37) produces

$$\begin{aligned}
 & \text{CRB}^{(b)}(u^0) = \text{CRB}^{(a)}(u^0) + \text{CRB}^{(a)}(u^0)Y^{(b)} \\
 & \quad \cdot (Z^{(b)} - Y^{(b)T}\Phi(Du^0)(\Phi^T(Du^0) \\
 & \quad \cdot X^{(b)}\Phi(Du^0))^{-1}\Phi^T(Du^0)Y^{(b)})^{-1} \\
 & \quad \cdot Y^{(b)T}\text{CRB}^{(a)}(u^0).
 \end{aligned} \tag{J1}$$

In addition, combining Eq. (C1) and inequality (C2) leads to

$$\begin{aligned}
 & Z^{(b)} - Y^{(b)T}\Phi(Du^0)(\Phi^T(Du^0)X^{(b)}\Phi(Du^0))^{-1} \\
 & \quad \cdot \Phi^T(Du^0)Y^{(b)} \geq Q_2^{-1},
 \end{aligned} \tag{J2}$$

which is equivalent to

$$\begin{aligned}
 & (Z^{(b)} - Y^{(b)T}\Phi(Du^0)(\Phi^T(Du^0)X^{(b)}\Phi(Du^0))^{-1} \\
 & \quad \cdot \Phi^T(Du^0)Y^{(b)})^{-1} \leq Q_2.
 \end{aligned} \tag{J3}$$

From Eqs. (J1) and inequality (J3) it can be readily obtained that

$$\begin{aligned} \mathbf{CRB}^{(b)}(\mathbf{u}^0) &\leq \mathbf{CRB}^{(a)}(\mathbf{u}^0) + \mathbf{CRB}^{(a)}(\mathbf{u}^0) \\ &\cdot \mathbf{Y}^{(b)} \mathbf{Q}_2 \mathbf{Y}^{(b)\top} \mathbf{CRB}^{(a)}(\mathbf{u}^0) \quad (\text{J4}) \\ &= \mathbf{MSE}(\hat{\mathbf{u}}_{\text{opt}}^{(1)}). \end{aligned}$$

### Appendix K: Proof of Proposition 12

It follows directly from Eqs. (48) and (52) that

$$\begin{aligned} &\mathbf{CRB}^{(c)}(\mathbf{u}^0) \mathbf{Y}^{(d)} (\mathbf{Z}^{(d)})^{-1} \\ &= \boldsymbol{\Phi}(\mathbf{D}\mathbf{u}^0) (\boldsymbol{\Phi}^\top(\mathbf{D}\mathbf{u}^0) (\mathbf{X}^{(d)} - \mathbf{Y}^{(d)} (\mathbf{Z}^{(d)})^{-1} \mathbf{Y}^{(d)\top}) \\ &\cdot \boldsymbol{\Phi}(\mathbf{D}\mathbf{u}^0))^{-1} \boldsymbol{\Phi}^\top(\mathbf{D}\mathbf{u}^0) \mathbf{Y}^{(d)} (\mathbf{Z}^{(d)})^{-1}. \quad (\text{K1}) \end{aligned}$$

Through some algebraic manipulations, we arrive at

$$\begin{aligned} &\mathbf{CRB}^{(c)}(\mathbf{u}^0) \cdot \mathbf{Y}^{(d)} (\mathbf{Z}^{(d)})^{-1} = \boldsymbol{\Phi}(\mathbf{D}\mathbf{u}^0) \\ &\cdot (\boldsymbol{\Phi}^\top(\mathbf{D}\mathbf{u}^0) \mathbf{X}^{(d)} \boldsymbol{\Phi}(\mathbf{D}\mathbf{u}^0))^{-1} \boldsymbol{\Phi}^\top(\mathbf{D}\mathbf{u}^0) \mathbf{Y}^{(d)} \\ &\cdot (\mathbf{Z}^{(d)} - \mathbf{Y}^{(d)\top} \boldsymbol{\Phi}(\mathbf{D}\mathbf{u}^0) (\boldsymbol{\Phi}^\top(\mathbf{D}\mathbf{u}^0) \mathbf{X}^{(d)} \boldsymbol{\Phi}(\mathbf{D}\mathbf{u}^0))^{-1} \\ &\cdot \boldsymbol{\Phi}^\top(\mathbf{D}\mathbf{u}^0) \mathbf{Y}^{(d)})^{-1}. \quad (\text{K2}) \end{aligned}$$

Substituting Eq. (K2) into Eq. (80) leads to

$$\begin{aligned} &\mathbf{MSE}(\hat{\mathbf{u}}_{\text{opt}}^{(2)}) \\ &= \mathbf{CRB}^{(c)}(\mathbf{u}^0) + \boldsymbol{\Phi}(\mathbf{D}\mathbf{u}^0) \\ &\cdot (\boldsymbol{\Phi}^\top(\mathbf{D}\mathbf{u}^0) \mathbf{X}^{(d)} \boldsymbol{\Phi}(\mathbf{D}\mathbf{u}^0))^{-1} \boldsymbol{\Phi}^\top(\mathbf{D}\mathbf{u}^0) \mathbf{Y}^{(d)} \\ &\cdot (\mathbf{Z}^{(d)} - \mathbf{Y}^{(d)\top} \boldsymbol{\Phi}(\mathbf{D}\mathbf{u}^0) (\boldsymbol{\Phi}^\top(\mathbf{D}\mathbf{u}^0) \mathbf{X}^{(d)} \boldsymbol{\Phi}(\mathbf{D}\mathbf{u}^0))^{-1} \\ &\cdot \boldsymbol{\Phi}^\top(\mathbf{D}\mathbf{u}^0) \mathbf{Y}^{(d)})^{-1} \mathbf{W}^{(d)\top} \mathbf{P}_2 \mathbf{W}^{(d)} \\ &\cdot (\mathbf{Z}^{(d)} - \mathbf{Y}^{(d)\top} \boldsymbol{\Phi}(\mathbf{D}\mathbf{u}^0) (\boldsymbol{\Phi}^\top(\mathbf{D}\mathbf{u}^0) \mathbf{X}^{(d)} \boldsymbol{\Phi}(\mathbf{D}\mathbf{u}^0))^{-1} \\ &\cdot \boldsymbol{\Phi}^\top(\mathbf{D}\mathbf{u}^0) \mathbf{Y}^{(d)-1} \mathbf{Y}^{(d)\top} \boldsymbol{\Phi}(\mathbf{D}\mathbf{u}^0) \\ &\cdot (\boldsymbol{\Phi}^\top(\mathbf{D}\mathbf{u}^0) \mathbf{X}^{(d)} \boldsymbol{\Phi}(\mathbf{D}\mathbf{u}^0))^{-1} \boldsymbol{\Phi}^\top(\mathbf{D}\mathbf{u}^0). \quad (\text{K3}) \end{aligned}$$

On the other hand, it can be seen from Eqs. (H3) and (H4) that

$$\begin{aligned} &\mathbf{CRB}^{(d)}(\mathbf{u}^0) - \mathbf{CRB}^{(c)}(\mathbf{u}^0) \\ &\leq \boldsymbol{\Phi}(\mathbf{D}\mathbf{u}^0) (\boldsymbol{\Phi}^\top(\mathbf{D}\mathbf{u}^0) \mathbf{X}^{(d)} \boldsymbol{\Phi}(\mathbf{D}\mathbf{u}^0))^{-1} \boldsymbol{\Phi}^\top(\mathbf{D}\mathbf{u}^0) \mathbf{Y}^{(d)} \\ &\cdot (\mathbf{Z}^{(d)} - \mathbf{Y}^{(d)\top} \boldsymbol{\Phi}(\mathbf{D}\mathbf{u}^0) (\boldsymbol{\Phi}^\top(\mathbf{D}\mathbf{u}^0) \mathbf{X}^{(d)} \boldsymbol{\Phi}(\mathbf{D}\mathbf{u}^0))^{-1} \\ &\cdot \boldsymbol{\Phi}^\top(\mathbf{D}\mathbf{u}^0) \mathbf{Y}^{(d)})^{-1} \mathbf{W}^{(d)\top} \mathbf{P}_2 \mathbf{W}^{(d)} \\ &\cdot (\mathbf{Z}^{(d)} - \mathbf{Y}^{(d)\top} \boldsymbol{\Phi}(\mathbf{D}\mathbf{u}^0) (\boldsymbol{\Phi}^\top(\mathbf{D}\mathbf{u}^0) \mathbf{X}^{(d)} \boldsymbol{\Phi}(\mathbf{D}\mathbf{u}^0))^{-1} \\ &\cdot \boldsymbol{\Phi}^\top(\mathbf{D}\mathbf{u}^0) \mathbf{Y}^{(d)-1} \mathbf{Y}^{(d)\top} \boldsymbol{\Phi}(\mathbf{D}\mathbf{u}^0) (\boldsymbol{\Phi}^\top(\mathbf{D}\mathbf{u}^0) \mathbf{X}^{(d)} \\ &\cdot \boldsymbol{\Phi}(\mathbf{D}\mathbf{u}^0))^{-1} \boldsymbol{\Phi}^\top(\mathbf{D}\mathbf{u}^0). \quad (\text{K4}) \end{aligned}$$

Combining Eqs. (K3) and inequality (K4), we have  $\mathbf{MSE}(\hat{\mathbf{u}}_{\text{opt}}^{(2)}) \geq \mathbf{CRB}^{(d)}(\mathbf{u}^0)$ , which completes the proof of Proposition 12.